17

Underwater Robots Part II: Existing Solutions and Open Issues

Lapierre Lionel
Laboratory of Informatics, Microelectronics and Robotics of Montpellier (LIRMM)
France

This paper constitutes the second part of a general overview of underwater robotics. The first part is titled: *Underwater Robots Part I: current systems and problem pose*. The works referenced as (Name*, year) have been already cited on the first part of the paper, and the details of these references can be found in the section 7 of the paper titled *Underwater Robots Part I: current systems and problem pose.* The mathematical notation used in this paper is defined in section 4 of the paper *Underwater Robots Part I: current systems and problem pose.*

1. Introduction

We propose in the sequel to introduce the existing solutions of the problems mentioned in the section 6 of the paper: *Underwater Robots Part I: current systems and problem pos*e. We will present the solutions that allows for guaranteeing the desired global performances exposed previously. Section 2 presents the solutions to the Modelling problems. Section 3 introduces the different navigation systems currently in used. Section 4 proposes an overview of the classic Guidance strategies, and point out the specificities of this Guidance system that allow solving various problems. Section 5 presents the Control solution, underlying the ones that exhibit guaranteed performances. The Mission Control, Software and hardware architectures problems will be briefly mentioned in section 6. Finally section 7 concludes this paper and section 8 presents de references used.

2. Naval architecture

This development assumes the *principle of superposition* that is, for most marine control application, a good approximation. These modelled phenomena are described in (Newmann, 1977), and for the most significant ones to underwater robotics, listed below.

2.1 Added Mass

The hydrodynamic forces due to added mass are a consequence of the kinetic energy exchanges between the system and the surrounding water. Consider an object moving with a strictly positive acceleration with respect to the surrounding fluid. The energy expense of the system is caused by the system inertial forces, and the inertial forces of the surrounding particles of water that has to be compensated in order to induce the movement. Thus, added

Source: Mobile Robots Towards New Applications, ISBN 3-86611-314-5, Edited by Aleksandar Lazinica, pp. 784, ARS/plV, Germany, December 2006

mass has an inertial incidence, as the system mass itself. In a situation of a strictly negative acceleration with respect to the surrounding fluid, the moving water particles will restore their kinetic energy to the system. The consequence is that the global apparent mass of an immerged object is bigger than its intrinsic- (or dry-) mass.
Notice that the added mass effect is a function of the fluid characteristics, the system geometry, and the body-frame-direction of the acceleration. Then, an immerged system will not have the same inertial behaviour – apparent mass – in all the directions, in opposition to the classic fundamental equation of the dynamics ($F = m \cdot a$), where the mass is not a function if the direction of the acceleration.
Moreover, the added mass forces are applied logically at the centre of gravity of the surrounding moving water. This point coincides with the system buoyancy centre, function of its geometry, while the dry-inertial effects impacts on the system centre of gravity.
The contribution from this added mass phenomena are mathematically expressed as:

$$\boldsymbol{\tau}_{\mathbf{A}} = -\mathbf{M}_{\mathbf{A}}\dot{\boldsymbol{\nu}} - \mathbf{C}_{\mathbf{A}}(\boldsymbol{\nu}) \cdot \boldsymbol{\nu}$$

As for the rigid body dynamics, it is advantageous to separate the added mass forces and moments in terms which belong to the added mass system 6x6 inertia matrix $\mathbf{M}_{\mathbf{A}}$ and the 6x6 matrix of hydrodynamic Coriolis and centripetal terms denoted $\mathbf{C}_{\mathbf{A}}(\boldsymbol{\nu}) \cdot \boldsymbol{\nu}$. To derive the expression of these two matrices, an energy approach based on Kirchhoff's equations is applied. The reader will find in (Fossen, 2002) and (Newmann, 1977) the detailed background material in order to estimate the added mass coefficients of a given object shape.

2.2 Hydrodynamic Damping

D'Alambert's paradox states that no hydrodynamic forces act on a solid moving completely submerged with constant velocity in a non-viscous fluid. In a viscous-fluid, frictional forces are present such that the system is not conservative with respect to energy (Fossen, 2002).
An object, immerged in a viscous fluid flow undergoes a force due to the relative velocity fluid/object, which can be decomposed with a component along the velocity direction, *the drag*, and a perpendicular second component, *the lift*, as depicted in Fig. 1. The origin of these forces is the non-isotropic repartition of the pressure around the object. Notice that a spherical or cylindrical object will only undergo a drag effect, since this geometry induces a symmetrical flow separation whatever the relative flow direction. Hence, for ROV-type vehicle, where isotropy is a sought factor, the lift effect is generally neglected. In the case of AUV-type vehicle, the control surfaces are using the lift effect to create a change in the direction of the robot velocity with respect to the fluid flow. Nevertheless, the main body of the AUV generally exhibits planes of symmetry that justify neglecting the lift effect. Thus, lift effect is generally modelled and considered in the actuation model, in order to evaluate the control surfaces action. The drag and lift effect are modelled as follows:

$$L = \frac{1}{2} \cdot \rho \cdot C_L \cdot A(\alpha) \cdot |v_t| \cdot v_t$$

$$D = \frac{1}{2} \cdot \rho \cdot C_D \cdot A(\alpha) \cdot |v_t| \cdot v_t$$

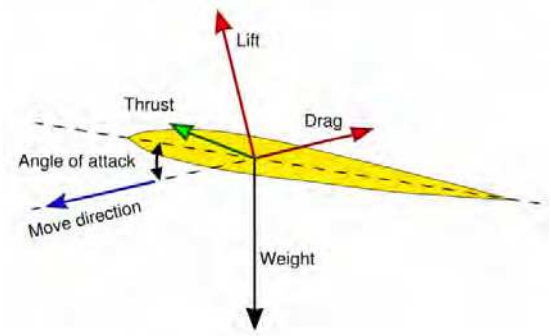

Fig. 1. Lift and Drag effects.

where L and D denote the lift and drag forces, respectively, ρ is the water density, α is the angle of attack, $A(\alpha)$ is the projected area perpendicularly to the flow direction and v_t is the relative fluid / object velocity. C_L and C_D are the lift and drag coefficients, respectively. These coefficients depends of the *Reynold number* of the immerged object, which is a function of the object geometry, the fluid density and the relative velocity, (Goldstein, 1976). The drag effect, as previously described is in fact the most significant hydrodynamic damping undergone by a robotics underwater system, and is specifically called *pressure drag*. Other damping related phenomena exist. The *skin friction* is due to the water viscosity and the object surface roughness. It induces a water 'sticking' effect that engenders a small drag phenomenon. This is generally neglected in the scope of underwater robotics applications. The *wave drift damping* can be interpreted as added resistance for surface vessels advancing in waves. Notice that, as stated for the added mass, the point of application of these forces is the system buoyancy centre. The reader will find in (Faltinsen, 1995) and (Newmann, 1977) detailed material to estimate the *Reynold number* and drag and lift coefficients.
Finally, the drag expressions acting on the 6 degrees of freedom of the solid are written as $\mathbf{D}(\mathbf{v})\cdot\mathbf{v}$, where $\mathbf{D}(\mathbf{v})$ is the 6×6 system damping matrix.

2.3 Restoring Forces

Beside the mass and damping forces, underwater systems and floating vessels will also be affected by gravity and buoyancy forces. In hydrodynamic terminology, the gravitational and buoyancy forces are called *restoring forces*, and they are equivalent to the spring forces in a *mass-spring-damper* system (Fossen, 2002). The gravity force or system weight, $W = \rho g$, where m denotes the system mass and g the acceleration of gravity, acts at the system gravity centre. The buoyancy force is expressed as $W = \rho \cdot g \cdot \nabla$ where ρ is the water density and ∇ is the volume of fluid displaced by the vehicle, and is applied at the volumetric centre (equivalently called buoyancy centre) of the displaced fluid. Notice that for a fully immerged solid the buoyancy centre coincides with the volumetric centre of the solid. Let $\mathbf{r}_g = [x_g \quad y_g \quad z_g]^T$ and $\mathbf{r}_b = [x_b \quad y_b \quad z_b]^T$ define the location of the gravity and buoyancy centres with respect to the origin of the body-frame {B}, respectively. Then, the 6×1 vector $\mathbf{G}(\boldsymbol{\eta})$ expressing the restoring forces along the 6 degrees of freedom of the system can be written as in equation (2).

$$\mathbf{G}(\boldsymbol{\eta}) = \begin{bmatrix} (W-B)\cdot\sin\theta \\ -(W-B)\cdot\cos\theta\cdot\sin\phi \\ -(W-B)\cdot\cos\theta\cdot\cos\phi \\ -(W\cdot y_g - B\cdot y_b)\cdot\cos\theta\cdot\cos\phi + (W\cdot z_g - B\cdot z_b)\cdot\cos\theta\cdot\sin\phi \\ (W\cdot z_g - B\cdot z_b)\cdot\sin\theta + (W\cdot x_g - B\cdot x_b)\cdot\cos\theta\cdot\cos\phi \\ -(W\cdot x_g - B\cdot x_b)\cdot\cos\theta\cdot\sin\phi - (W\cdot y_g - B\cdot y_b)\cdot\sin\theta \end{bmatrix} \quad (2)$$

In addition to the restoring forces $\mathbf{G}(\boldsymbol{\eta})$, the system can be equipped with ballasts allowing for pumping water in order to modify the system weight, and as a consequence, the location of the gravity centre. Hence $\mathbf{r}_g$ and W become controllable variables that allows for heave, pitch and roll dynamic stabilisation, for surface or semi-submersible vessels, depending on the number and the location of the ballast tanks (Faltinsen, 1995). Notice that underwater Glider systems are using this ballast control to alternate a the gravity / buoyancy dominancy in order to create a descending / ascending forces that induce a water flow in which the system flies.

2.4 Environmental disturbances

Environmental disturbances, due to waves, wind and ocean currents have a significant impact on marine system dynamics. Simple models for these disturbances applicable to control system design are found in (Fossen, 2002) and (Prado, 2004). A more general discussion on marine hydrodynamics is presented in (Faltinsen, 1995) and (Newmann, 1977). Notice that wave and wind effects have an effective incidence on surface and sub-surface ASCs, and UUVs shallow water application.

Winds affect surface vessels and their consideration is necessary for designing large crude carriers and tankers auto-pilots. ASCs are generally designed in such a way that wind resistance is negligible, but (Neal, 2006) is presenting an interesting study on a small-scaled sailing ASC and demonstrates the feasibility and interest of such a system.

Waves are induced by many factors: wind, tide, storm surges and *Stokes* drift. A linear propagating wave theory is derived, borrowing from potential theory and Bernouilli's equations. It allows for a statistical description of wave based on an estimated wave spectrum. The wave elevation, ξ_z, of a long-crested irregular sea propagating along the positive x-axis can be written as the sum of a large number of wave components, i.e.:

$$\xi_z = \sum_{j=1}^{n} A_j \cdot \sin\left(\omega_j \cdot t - k_j \cdot x + \varepsilon_j\right)$$

Where A_j, ω_j, k_j and ε_j are respectively the wave amplitude, circular frequency, wave number and random phase angle of wave component *j*. The random phase angles ε_j are uniformly distributed between 0 and 2π and constant with time. The wave amplitude A_j is distributed according to a wave spectrum estimated from wave measurements. Recommended sea spectra from ISCC (International Ship and Offshore Structures Congree) and ITTC (International Towing Tank Conference) are often used to calculate A_j (Faltinsen, 1995). Underwater, ω_j and k_j are related with a dispersion relationship that rapidly attenuates the wave effects with depth. This attenuation effect is clearly stated in the expression of the horizontal fluid velocity $\dot{\xi}_x$ and acceleration $\ddot{\xi}_x$:

$$\dot{\xi}_x = \sum_{j=1}^{n} \omega_j \cdot A_j \cdot e^{-k_j z} \sin\left(\omega_j \cdot t - k_j \cdot x + \varepsilon_j\right)$$

$$\ddot{\xi}_x = \sum_{j=1}^{n} \omega_j^2 \cdot A_j \cdot e^{-k_j z} \cos\left(\omega_j \cdot t - k_j \cdot x + \varepsilon_j\right)$$

The wave-induced velocity and acceleration vectors of the surrounding particles of fluid are expressed as $\dot{\boldsymbol{\xi}}$ and $\ddot{\boldsymbol{\xi}}$.

The wave-induced oscillatory disturbance is rapidly attenuated with the depth, and in most UUVs application is neglected. But, ocean current is more problematic. Ocean current are horizontal and vertical circulation systems of ocean waters produced by tides, local wind, *Stokes* drift major ocean circulation, storm surges and strong density jumps in the upper ocean (combined action of surface heat exchange and salinity changes). As for the wave effect, ocean current induces on an immerged object a hydrodynamic load, due to the externally-induced movement of the surrounding particles of water. The low dynamic of the phenomena justifies assuming that the current is slowly-varying, hence the current velocity vector ς, expressed in the universal frame {*U*} is considered as constant.

Then the wave and ocean current induced disturbances are modelled as the universal velocity $\boldsymbol{\nu}_{\mathbf{w}}$ and acceleration $\dot{\boldsymbol{\nu}}_{\mathbf{w}}$ of the surrounding fluid. Expressed in the body frame {*B*}, it comes:

$$\boldsymbol{\nu}_{\mathbf{w}} = \mathbf{R} \cdot \left(\dot{\boldsymbol{\xi}} + \varsigma\right)$$

$$\dot{\boldsymbol{\nu}}_{\mathbf{w}} = \mathbf{R} \cdot \ddot{\boldsymbol{\xi}} + \dot{\mathbf{R}} \cdot \left(\dot{\boldsymbol{\xi}} + \varsigma\right)$$

Finally, considering the previously described environmental disturbances, the external disturbances acting on an immerged vehicle are expressed by the 6×1 vector **w**:

$$\mathbf{w} = \mathbf{M}_A(\boldsymbol{\eta}) \cdot \dot{\boldsymbol{\nu}}_w + \mathbf{C}_A(\boldsymbol{\nu}_w) \cdot \boldsymbol{\nu}_w + \mathbf{D}(\boldsymbol{\nu}_w) \cdot \boldsymbol{\nu}_w$$

Considering the superposition principle, this formalism allows for modelling the hydrodynamic forces that the system will undergo, in function of the system states $\boldsymbol{\eta}$ and $\boldsymbol{\nu}$. A Newton-Euler analysis or a Lagrangian-type derivation allows for writing the equations of motion for an underwater robot without manipulator as follows (Fossen, 2002) and (Lapierre *et al.*, 1998):

$$\begin{aligned} \dot{\boldsymbol{\eta}} &= \mathbf{K}(\boldsymbol{\eta}) \cdot \boldsymbol{\nu} \\ \mathbf{M}(\boldsymbol{\eta}) \cdot \dot{\boldsymbol{\nu}} + \mathbf{C}(\boldsymbol{\nu}) \cdot \boldsymbol{\nu} + \mathbf{D}(\boldsymbol{\nu}) \cdot \boldsymbol{\nu} + \mathbf{G}(\boldsymbol{\eta}) &= \boldsymbol{\tau} + \mathbf{w} \\ \boldsymbol{\tau} &= \mathbf{B} \cdot \mathbf{u} \end{aligned} \tag{3}$$

where the kinematic relation is written as:

$$\mathbf{K}(\boldsymbol{\eta}) = \begin{bmatrix} \cos\psi \cdot \cos\theta & -\sin\psi \cdot \cos\phi + \cos\psi \cdot \sin\theta \cdot \sin\phi & \sin\psi \cdot \sin\phi + \cos\psi \cdot \sin\theta \cdot \cos\phi & 0 & 0 & 0 \\ \sin\psi \cdot \cos\theta & \cos\psi \cdot \cos\theta + \sin\psi \cdot \sin\theta \cdot \sin\phi & -\cos\psi \cdot \sin\phi + \sin\psi \cdot \sin\theta \cdot \cos\phi & 0 & 0 & 0 \\ -\sin\theta & \cos\theta \cdot \sin\phi & \cos\theta \cdot \cos\phi & 0 & 0 & 0 \\ 0 & 0 & 0 & 1 & \sin\phi \cdot \tan\theta & \cos\phi \cdot \tan\theta \\ 0 & 0 & 0 & 0 & \cos\phi & -\sin\phi \\ 0 & 0 & 0 & 0 & \dfrac{\sin\phi}{\cos\theta} & \dfrac{\cos\phi}{\cos\theta} \end{bmatrix} \tag{4}$$

M denotes the 6x6 symmetric inertia matrix as the sum of the diagonal rigid body inertia matrix and the hydrodynamic added mass matrix $\mathbf{M_A}$, **C(v)** is the 6×6 Coriolis and centripetal matrix including rigid-body terms and terms $\mathbf{C_A(v)}$ due to added mass, D(v) is the 6×6 damping matrix

including terms due to drag forces, $\mathbf{G}(\boldsymbol{\eta})$ is a 6x1 vector containing restoring terms formed by the vehicle buoyancy and gravitational terms and $\mathbf{w}$ is the 6x1 vector representing the environmental forces and moments (e.g. wave and current) acting on the vehicle.
The actuation input $\mathbf{u}$ is composed with the thrusters' propeller angular velocity and the desired angle of the control surfaces. Thrusters' dynamics are nonlinear and quite complex. The reader will find in (Yuh, 2000), (Whitcomb and Yoerger, 1995), and the references therein, experimental elements to compare four thrusters models for blade-propeller type underwater thrusters driven by brushless DC motor. Control surfaces are using the lift effect to act on the system. Approximated theoretical solutions and experimental data have been collected to produce efficient models reported in (Fossen, 2002) and (Aucher, 1981). Notice that Equation (3) expresses a linear relation between $\boldsymbol{\tau}$ and $\mathbf{u}$. This approximation is justified under the assumption that the thruster's dynamics have much smaller time constants than the vehicle dynamics [YUH]. Nevertheless, for control surfaces neglecting second order terms might be far from reality. Moreover, control surfaces are undergoing heavy hydrodynamic reaction forces, inducing deformations and a decrease in the drive motor response.
The constant physical parameters of the actuation model compose the $\mathbf{B}$ matrix**.** Its components are dependent on each robot's configuration, control surfaces, ballast system, number and location of thrusters. Therefore $\mathbf{B}$ is generally not a diagonal, even square matrix.
The environmental disturbance, $\mathbf{w}$, induces a dynamic load on the system that can be considered during the control design, since many of these effects are suppressed in the closed loop. Moreover, ocean current induces on the system a static inertial-based load that modifies the working condition of thrusters and, as we will see later confronts an under-actuated system (ASC, AUV) with the Brocket's limitations (Brockett*, 1983) and impedes it to realize a pose stabilisation with a desired heading.
When one or more manipulators are attached to the vehicle, it becomes a multi-body system and modelling becomes more complicated. The effects of the hydrodynamics on each link of the manipulators on vehicle motion have to be considered. Moreover, underwater manipulation requires the manipulator end-effector to exert a desired force on the structure on which the intervention is performed. Hence, the modelling has to explicitly consider the effects of the environment reaction on the system. Using the fact that intervention is done while the vehicle is station-keeping, the system model is simplified and decoupled (Whitcomb*, 2000), (Lapierre[a] *et al.*, 1998) and (Fraisse *et al.*, 2000).

2.5 Biological Inspired system: theory of locomotion

During a movement, fishes are continuously adjusting their body-shape in order to locally control the fluid flow along their body, hence reaching high efficiency in the thrust generation. This continuous deformation is difficult to model, and general modelling solutions consider a hyper-redundant N-serially-linked segments system. The purpose of the dynamic model is to express the actuation effects on the system states evolution. Then, the control analysis allows for designing an actuation pattern (also called *gait*) that "wiggles" the body surface in order to generate the desired thrust. The relationship between shape and position changes requires mathematical analysis borrowing from fluid potential theory and Lie algebra (Sfakiotakis & Tsakiris, 2004). Notice the use of Lagrange multiplier technique with tensor notation, to obtain a solution of the dynamic model of an eel-like system (McIsaac & Ostrowski, 2002).

The physical constant parameters of the dynamic model (2) can be estimated using graphics in the literature. The dynamic parameters can also be precisely identified with hydrodynamic Tank Tests, reproducing an artificial fluid flow on the immerged structure, connected to a force sensor that allows for measuring the 6 forces and torques induced by the flow. Nevertheless, despite the precision of the model-parameters estimation, the modelling error has a significant impact on the control performances. Let $\mathbf{P}$ be the vector of the system dynamic parameters, $\hat{\mathbf{P}}$ is an estimation of $\mathbf{P}$ and $\tilde{\mathbf{P}} = \mathbf{P} - \hat{\mathbf{P}}$ denotes the modelling error. The control robustness denotes the system ability to react as desired, despite $\tilde{\mathbf{P}}$. Moreover, the previous modelled phenomena expressions assume that the neglected high order terms induce minor effect. This might be empirically verified, but the theoretical consideration of the effects of the *unmodelled dynamics* is still an opened issue. This unmodelled dynamics has also another interest. Indeed, an accurate modelling that explicitly considers the high order terms will result in a precise description of the system dynamics, allowing for fine simulations. Nevertheless, modelling does not imply controllability, and as we will see in the sequel, the control design will impose to neglect some problematic coupled and non-linear terms of the model.

3. Navigation System

The Navigation System provides estimates of the vehicle states based on a set of motion sensor suites.
As underwater systems have been developed, the complexity of the navigation problem increased. The demands are different in function of the system application. An ASC is riding the sea surface, and the navigation problem is to constantly estimate its global position with respect to the pre-defined geo-referenced route. The possibility to directly use GPS information and long-range radio link greatly simplifies the problem. A ROV navigation system will be tasked with estimating the necessary information in order to insure a robust and precise hovering control in front of the target on which the manipulation is performed. The approach phase requires similar information than for AUV, in order to control the system movement on a globally-defined or terrain-based route. Then, the navigation problem for UUVs is related with the estimation of the necessary information in order to accomplish the 3 following types of objectives:

- terrain-based pose-stabilisation ,
- terrain-based route following,
- globally-defined route following.

Underwater, the absence of direct GPS measurements leads different alternatives:

- periodic surfacing,
- pure dead-reckoning navigation,
- calibrated-acoustic-devices based navigation,
- terrain-based and SLAM navigation.

In any case, multiple sensors are needed in order to provide a set of sufficient measurements to estimate $\hat{\boldsymbol{\eta}}$ and $\hat{\boldsymbol{\nu}}$. UUV sensor suite is generally redundant, different sensors providing an estimation of the same physical quantity. Moreover, measurements related to the UUV movements are linked with the differential relation of the laws of mechanics. The navigation system is tasked with the fusion of these measurements in order to provide the best estimate of the system states.
As mentioned in (Pascoal *et al.*, 2000 and Oliveira, 2002) navigation system is traditionally done in a stochastic setting using *Kalman-Bucy* filtering theory (Brown & Hwang, 1992). The UUV situation

leads to consider nonlinear systems, and navigation solutions are usually sought by resorting to *Extended Kalman* filtering techniques. The stochastic setting requires a complete parameterization of process and observation noise, a task that may be difficult, costly, or not suited to the problem in hand. This issue is argued at length in (Brown & Hwang, 1972), where the author points out that in a great number of practical applications the filter design process is entirely dominated by constraints that are naturally imposed by the sensor bandwidth. In this case, a design method that explicitly addresses the problem of merging information provided by a given sensor suite over distinct, yet complementary frequency regions is warranted.

Complementary filters have been developed to address this issue explicitly (Oliveira, 2002). In the case where the navigation sensors can be sampled at the same period, the corresponding filter operators are linear and time-invariant. This leads to a fruitful interpretation of the filters in the frequency domain, as briefly described in Fig. 2, in the situation of heading estimation.

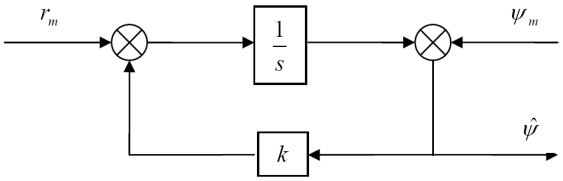

Fig. 2. complementary filter estimating the yaw angle $\hat{\psi}$ based on the measurements of the yaw-rate ψ_m and the yaw angle r_m, from (Pascoal *et al.*, 2000).

Straightforward computation allows for writing the filter structure of Fig. 2 as:

$$\hat{\psi}(s) = \underbrace{\frac{k}{s+k}}_{T_1(s)} \cdot \psi_m(s) + \underbrace{\frac{1}{s+k}}_{T_2(s)} \cdot r_m(s)$$

where the subscript $(\cdot)_m$ denotes the measurement, and $\hat{\psi}(s)$, $\psi_m(s)$ and $r_m(s)$ are the *Laplace* transform of $\hat{\psi}$, ψ_m and r_m, respectively. Notice the following important properties:

I $T_1(s)$ is low pass, the filter relies on information provided by the compass at low frequency only.

ii $T_2(s) = I - T_1(s)$. The filter blends the information provided by the compass in the low frequency region with that available form the rate gyro in the complementary region.

iii The break frequency is simply determined by the choice of the parameter k.

The frequency decomposition induced by the complementary filter structure holds the key of its practical success, since it mimics the natural frequency decomposition induced by the physical nature of the sensors themselves. Compasses provide reliable information at low frequency only, whereas rate gyros exhibit biases and drift phenomena in the same frequency region and therefore useful at higher frequencies. Complementary filter design is then reduced to the choice of k so as to meet a target break frequency that is entirely dictated by the physical characteristic of the sensors. From this point of view, this is in contrast with a stochastic approach that relies heavily on a correct description of process and measurement noise (Brown, 1972).

In the case of linear position, based on low-rate acoustically relayed global measurements, and acceleration estimation based on some onboard accelerometers, the navigation system

has to merge inertial frame position with body-axis accelerations. This explicitly introduces the nonlinear rotation matrix **R** from inertial to body-axis in the filter structure. The resulting nonlinear filter is cast in the framework of Linear Parametrically time-Varying systems (LPVs). Using this set-up, filter performance and stability are studied in an H_∞ setting by resorting to the theory of Linear Matrix Inequalities (LMIs, Boyd *et al.*, 1994).

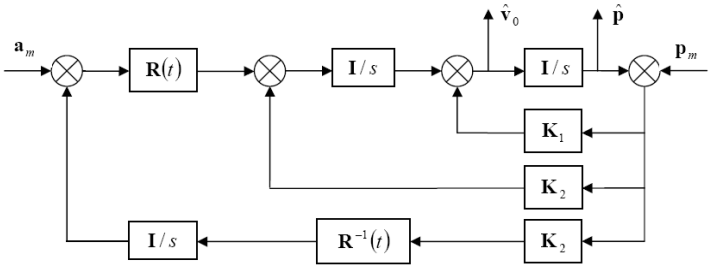

Fig. 3. complementary filter estimating the inertial position $\hat{\mathbf{p}}$ and velocity $\hat{\mathbf{v}}_0$ based on the measurements of the body-frame accelerations $\mathbf{a}_m$ and the inertial position $\mathbf{p}_m$ from (Pascoal ***et al.***, 2000).

Fig. 3 describes a filter that complements position information with that available from onboard accelerometers, where $\mathbf{a}_m = [\dot{u}_m \quad \dot{v}_m \quad \dot{w}_m]^T$ denotes the measured linear accelerations along the 3 body-axis, $\mathbf{p}_m = [x_m \quad y_m \quad z_m]^T$ is the measured absolute position, $\hat{\mathbf{v}}_0 = [\hat{\dot{x}} \quad \hat{\dot{y}} \quad \hat{\dot{z}}]$ is the inertial estimated velocity and $\hat{\mathbf{p}}$ is the estimated geo-referenced position. The structure design is then reduced to the choice of the gain matrices $\mathbf{K}_1$, $\mathbf{K}_2$ and $\mathbf{K}_3$. (Pascoal *et al.*, 2000) is converting the problem of filter design and analysis into that of determining the feasibility of the related set of Linear Matrix Inequalities. As a consequence, the stability of the resulting filters as well as their frequency-like performance can be assessed using numerical analysis tools that borrow from convex optimisation techniques (Boyd *et al.*, 1994 and Brown 1972).

Despite the time-varying problem, the characteristics of the sound channel imply that the position measurements are available at a rate that is lower than that of the velocity or acceleration sensors. To deal with this problem, (Oliveira, 2002) proposes an approach to navigation system design that relies on multi-rate *Kalman* filtering theory. Moreover, the author introduces some analysis tools to show that multi-rate filters can be viewed as input-output operators exhibiting "frequency-like" properties that are natural generalization of those obtained for the single rate case.

The filter of Fig. 3 proposes an interesting combination for the pose-stabilisation problem. Suppose a vision system providing an estimation of the relative position between a ROV and a visible landmark located on the structure onto which a manipulation has to be performed. The accelerometers and the vision system, equipped with appropriate feature extraction algorithms, provide precise necessary information to complete a hovering manoeuvre. (Kaminer *et al.*, 2001) provides the detailed solution to this problem, applied to the problem of estimating the relative position and velocity of an autonomous aircraft with respect to a moving platform, such as a naval landing vessel. This solution allows fusing accelerometers measurements with information coming from the image space, using an adequate vision system. The consequence is the injection in the filter structure of the vision

sensor model, as depicted in Fig. 4. **Fig. 4**, where $\mathbf{p}_m^{\mathrm{Im}}$ denotes the image coordinates of the desired feature, $\mathbf{R}_U^{Cam}(t)$ is the rotation matrix from the universal frame to the camera frame, h_θ is the calibrated vision-system model, expressing the relative position of the desired feature in the image frame $\mathbf{p}_m^{\mathrm{Im}}$ from the relative feature position expressed in the camera frame and H^T is the Jacobian matrix of h_θ.

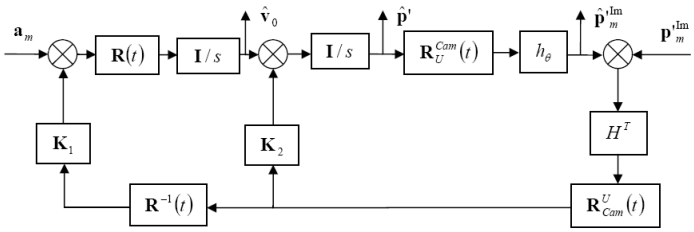

Fig. 4. complementary filter estimating the relative position of the desired feature with the UUV $\hat{\mathbf{p}}'$ and velocity $\hat{\mathbf{v}}_0$ based on the measurements of the body-frame accelerations $\mathbf{a}_m$ and the position of the desired feature in the image plane, $\mathbf{p}'^{\mathrm{Im}}_m$ from (Kaminer ***et al.***, 2001).

Moreover, the authors of (Kaminer *et al.*, 2001) show that the resulting filter exhibits guaranteed performances, that is:

$$\text{If } \left|\mathbf{p}'^{\mathrm{Im}}\text{-}\mathbf{p}'^{\mathrm{Im}}_m\right| < \zeta_p \text{ and } \left|\mathbf{a}\text{-}\mathbf{a}_m\right| < \zeta_a, \exists \boldsymbol{\varepsilon}, \text{such that } \tilde{\mathbf{p}}' = \mathbf{p}' - \hat{\mathbf{p}}' < \boldsymbol{\varepsilon}$$

where ζ_p is a bound on the measurement error, related with the sensor accuracy. The feasibility test, required for the choice of the gain matrices $\mathbf{K}_1$, $\mathbf{K}_2$ and $\mathbf{K}_3$, can be iterated order to minimize the guaranteed bound $\boldsymbol{\varepsilon}$, (Silvestre, 2000). An interesting unsolved question is related to the inverse problem: given a necessary $\boldsymbol{\varepsilon}$, what should be the sensors characteristics, in terms of sampling frequency and accuracy, that provide an estimation guaranteed to be within $\boldsymbol{\varepsilon}$.

A generalisation of the previous results allows to state that, given a complete sensor suite that provides $\boldsymbol{\eta}_m$ and $\boldsymbol{\nu}_m$, a combination of different complementary filters is able to provide an estimation of the system states such that:

$$\text{If } \left|\boldsymbol{\eta}\text{-}\boldsymbol{\eta}_m\right| < \zeta_\eta \text{ and } \left|\boldsymbol{\nu}\text{-}\boldsymbol{\nu}_m\right| < \zeta_\nu, \exists\left(\boldsymbol{\varepsilon}_\eta, \boldsymbol{\varepsilon}_\nu\right), \text{such that } \tilde{\boldsymbol{\eta}} = \boldsymbol{\eta} - \hat{\boldsymbol{\eta}} < \boldsymbol{\varepsilon}_\eta \text{ and } \tilde{\boldsymbol{\nu}} = \boldsymbol{\nu} - \hat{\boldsymbol{\nu}} < \boldsymbol{\varepsilon}_\eta,$$

that is, the navigation system is exhibiting guaranteed performance. Notice that the condition $\left|\boldsymbol{\eta}\text{-}\boldsymbol{\eta}_m\right| < \zeta_\eta$ imposes the system to be equipped with appropriate sensors, including a device able to provide an estimation of the global position of the system, or at least able to counter-balance the systematic growth of the positioning error, induced by dead-reckoning navigation. As we have already suggested, a solution is to associate with the immerged system a calibrated reference device that is acoustically relaying the GPS information to the system. Being statically immerged, moored, drifting, or actuated, the use of these calibrated references greatly increases the operational and logistic burdens and its efficiency is dependant on the quality of the acoustic link. Terrain-based navigation offers a precious complement of information. Indeed a remarkable terrain feature can be used as a reference point in order to precisely estimate displacement.

Moreover, if this benchmark has been previously spotted and geo-referenced, then terrain navigation offers sufficient information in order to meet the guaranteed performance requirement, by exploiting the geometric and morphological characteristics of the environment; in particular sea bottom features such bathymetry, spatial distribution of biotypes distribution. This technique is named Simultaneous Localisation And Mapping (SLAM) and is currently an active topic of research (Leonard *et al.**, 2002, Nettleton *et al.*, 2000 and Rolfes & Rendas, 2001). The key point here is to guarantee the data association providing an unambiguous recognition of the spotted landmark. This implies to choose features that are robust with respect to the point of view (William *et al.**, 2002), which is a difficult problem. Indeed a wrong data association can drive the vehicle in a situation where it could be lost, justifying the necessity of combining both navigation strategies, using calibrated acoustic relays and terrain-based navigation. Notice that the SLAM aided navigation goal is not to produce a complete and globally consistent map of the environment, but only to provide sufficient environment knowledge in order to estimate, with the desired accuracy, the system displacement. Then the considered maps consist of a few number of relevant spatially features. In this way, the complexity of the filtering / estimation problem is limited and the map-data association is robustly solved (Rolfes & Rendas, 2001). The data-association is generally solved within a stochastic framework, estimating the result of the data association in confronting a representation of the posterior densities to the current sensors information, in order to predict the uncertainty of a given association attempt. *Extended Kalman* and *Monte Carlo* techniques are currently being used to solve this problem (Nieto *et al.*, 2003).

The particular problem of local coordinated navigation of an underwater vehicles flotilla can be elegantly posed using the multi-SLAM technique (Reece & Roberts*, 2005). As for a single vehicle, local coordinated navigation requires the estimation of the necessary information in order to guaranty the movement control of the group. As suggested before, ASC relaying geo-referenced information to the immerged vehicles is greatly helpful. Moreover, since the best communication rate is performed in the vertical water column, this vehicle can also be in charge of insuring the inter-vehicle communication. Nevertheless, the sea surface is not free of obstacle and it is expected that the ASC has to temporarily deviate form its nominal trajectory, thus compromising the communication net. Then, the immerged system has to share other kind of common references. SLAM technique offers interesting alternative to the centralized communication situation, and underlines the problem of extracting terrain-features that are robust with respect to the point of view. The sea bottom, at a given instant is a common reference for all the fleet members, and can greatly helps the relative localisation estimation. This implies that the vehicles are able to exchange information, which could be performed via the surface vessel. An alternative is to use a sub-surface system that can benefit from its vertical actuation in order to avoid obstacle without deviating form its nominal horizontal path. Moreover, this underwater system can adjust its immersion in order to optimize the acoustic cover on top of the flotilla. Nevertheless, despite the poor-rate horizontal communication capabilities, the possibility of a direct communication between two members cannot be neglected. Moreover, a precise temporal synchronization of all the fleet members allows for estimating the distance between the emitter and the receiver. That is precious information concerning the flotilla internal states. Moreover, in this context, an AUV can relay information to another one, which could be unreachable from the (sub-)surface vehicle. Inter-members communication implies to minimize the sum of the necessary information to exchange. In (Lapierre[c] *et al.**, 2003) it has been shown that the collaboration between two underwater vehicles following the same horizontally shifted paths requires, besides the local navigation data, the mutual exchange

of the current control objective of both the vehicles. That is the current path-point each of them is currently tracking. The extension of this solution to N vehicles is still opened. The occurrence on an obstacle induces for the concerned vehicles to deviate from their respective paths. This may imply a reaction on the entire flotilla members, in order to keep the cohesion on the formation and insure a smooth return to a nominal situation. This necessary behaviour requires having regular information about the distance between the vehicles. A robust estimator of these distances has to fuse the (quasi-)global positioning estimation from the (sub-)surface vehicle with the estimation of the relative distance extracted from a measurement of the time-of-flight of the signal along the communication channel. Notice how a precise temporal synchronisation solves trivially the distance estimation. Complementary filters seem to be well suited to this problem, and the guaranteed performance they are offering is of major interest in this application. Fusing all the information related to the acoustical distance between each member towards all, with the one coming from the (sub-)surface vehicle, in considering the erratic sampling rates, is an exciting opened issue.

4. Guidance

The Guidance System processes Navigation/Inertial reference trajectory data and output set-points for desired vehicle's velocity and attitude.

In ROV systems, guidance commands are sent from a ground or mother-boat station, while AUVs have an onboard guidance processor. With regard to this, a guidance system plays the vital role in bringing autonomy to the system (Naeem *et al.*, 2003). The guidance system computes the best approach to be followed by the vehicle, based on the target location, joy-stick operator inputs (if any), external inputs (weather data), Earth topological information, obstacle and collision avoidance data, and finally the state vector which is available as output from the navigation system (Fossen, 2002). Guidance system for underactuated marine vessels is usually used to generate a reference trajectory for time-varying trajectory-tracking or time-invariant manoeuvring for path-following. As a guide-line example, we have chosen to consider the guidance problem for path-following. The underlying assumption in path-following strategy is that the vehicle's forward speed tracks a desired speed profile, while the controller acts on the vehicle orientation to drive it to the path. Thus, as we will see in the sequel, the guidance problem for underactuated vehicles is reduced to the strategy in driving the desired heading angle of the system (ψ_d), while the desired forward velocity (u_d) is left to the arbitrary choice of the mission designer.

4.1 Set-point regulation

A rudimentary guidance system, of general use for marine vessels, is called Set-point regulation. This is a special case where the desired velocity, position, and attitude are chosen to be constant. Applied to a surface craft, the desired attitude is reduced to the desired heading the vehicle has to follow. Then a desired pattern-following (in order to achieve a bottom acoustic coverage for example) will require from the guidance system a collection of n set-points defined by the three following characteristics: desired forward velocity, desired heading and duration, defining an element of the set-point database as: $(U_k \quad \psi_k \quad t_k)^T$, for k=1,…,n. Notice that the environmental information is of major importance for this type of guidance system. Indeed the presence of a lateral current or wind will impact on the system trajectory without being compensated, resulting in a distorted achieved pattern. Nevertheless, this is the simplest guidance, and limited weather

condition is enough to achieve simple missions as acoustic coverage of the seabed, since the acquired data will be post-processed.

4.2 Way-point guidance

Systems for Way-point Guidance are used both for ship and underwater vehicle. The system consists of a way-point generator with the human interface. The selected way-point are defined using Cartesian coordinated $(x_k \quad y_k \quad z_k)^T$ for k=0,…,n, and stored in a way-point database. In the case where the path is only specified in the horizontal plane, only the two coordinates $(x_k \quad y_k)^T$ are used. Additionally, other way-point properties like speed (U_k), heading (ψ_k) etc, can be defined. For surface vessels, this means that the ship should pass through way-point k at forward speed U_k with heading angle ψ_k. The heading is usually unspecified during cross-tracking, whereas it is more important during a crab-wise manoeuvre close to offshore installation, with the condition that the vehicle carries lateral thrusters in order to achieve the dynamic positioning. The way point database can be generated using many criteria, (Fossen, 2002):

- Mission: the vessel should move from some starting point $(x_0 \quad y_0 \quad z_0)^T$ to the terminal $(x_n \quad y_n \quad z_n)^T$, via the way-points $(x_k \quad y_k \quad z_k)^T$.
- Environmental data: information about wind, waves, current can be used for energy optimal routing (or avoidance of bad weather for surface vessels).
- Geographical data: information about shallow waters, islands etc, should be included.
- Obstacles: floating constructions and other obstacles must be avoided.
- Collision Avoidance: avoiding moving vessels close to the defined route by introducing safety margins.
- Feasibility: each way-point must be feasible, in that it must be possible to manoeuvre to the next way-point without exceeding maximum speed, turning rate etc.

On-line replanning can be used to update the way-point database in case of time-varying conditions like changing weather, moving vessels, etc. In practice, the way-point guidance strategy can be cast in the set-point regulation description, in computing the current set-point characteristics in function of the currently tracked way-point k, and the system position, thanks to the following trivial computation:

$$\psi_k = \arctan\left(\frac{x_k - x}{y_k - y}\right) \tag{5}$$

and U_k is left to the arbitrary choice of the operator. This solution constantly adjusts the desired vehicle heading toward the location of the way-point k. This techniques requires the definition of a threshold d_{wp}, under which the vehicle is considered to be in an acceptable vicinity of the way-point k, and allows for iterating the process to the next waypoint k+1.

Another option is to define a followable path, based on the way-point location. It is common to represent the desired path using straight lines and circles arc to connect the way-points (cf. Fig. 5 – dashed line). The drawback of this method, shared by the previous one, is that a jump in the desired yaw-rate r_d is experienced. This is due to the fact that the desired yaw-rate along the straight lines is $r_d=0$ while r_d =constant on the circle arc. Hence introducing a jump in the desired yaw-rate during transition from straight line to circle arc, or between consecutive way-points. This produces a small off-set during cross-tracking.

Cubic spline generated path results in a smoother reference and this drawback is overcome (cf. Fig. 5 – solid line).

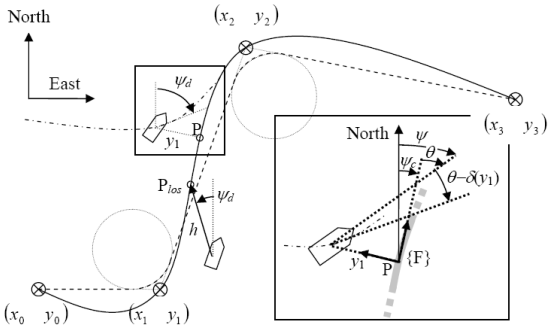

Fig. 5. the path is generated using straight lines and circle arcs – dashed line - or using cubic spline interpolation – solid line. Line of Sight and Nonlinear Approach guidance problem pose.

The path-following guidance strategy requires the definition of a more complex setting, introducing the problem of the path parameterization and the choice of the target-point to be tracked on the path.

4.3 Line of Sight

The Line Of Sight (LOS) strategy is an extension of the way-point guidance described in Equation (5), where the target point is not located onto the next way-point, but defined as the intersection between the path and the LOS vector of length h (horizon). The coordinates $(x_{los} \quad y_{los})$ of the target point P_{los} (cf. Fig. 5) can be easily computed in solving the following equations:

$$(y_{los} - y)^2 + (x_{los} - x)^2 = h^2$$

$$\left(\frac{y_{los} - y_{k-1}}{y_{los} - y_{k-1}}\right) = \left(\frac{y_k - y_{k-1}}{y_k - y_{k-1}}\right) = \text{constant}$$

Notice that this is solvable if and only if $h>y_1$, where y_1 is the cross-tracking error, that is the distance between the robot and the closest point on the path. The two previous equations have two solutions, and a contextual analysis allows for removing this ambiguity.

A more general solution of the guidance problem, originally proposed in (Samson & Ait-Abderrahim, 1991), is the **Nonlinear Approach Guidance** strategy. It is based on the consideration of a Serret-Frenet frame {*F*}, attached to the closest point on the path P. Consider Fig. 5, let ψ_c define the absolute angle of the tangent to the path at point P, and let $\theta = \psi - \psi_c$ be the variable that the control system should reduce to 0 as y_1 vanishes. This desired evolution of θ is captured in the definition of the approach angle $\delta(y_1)$:

$$\delta(y_1) = -\theta_a \cdot \tanh(k_\delta \cdot y_1) \tag{6}$$

where k_δ is a positive gain and $0 < \theta_a \le \pi/2$ defines the asymptotic approach. That is when y_1 is big, the desired angular incidence to the path is θ_a, maximally defined as $\pi/2$ and inducing the desired approach to directly point toward P. As y_1 is reducing $\delta(y_1)$ decreases, down to 0 when

the cross-tracking error is null. This method offers a smooth manoeuvre toward the path and, moreover, defines an appropriate framework in order to derive the control expression using of *Lyapunov* techniques. The global objective of the control is then to reduce the quantity $\theta - \delta(y_1)$ to zero. Nevertheless, this method has a major drawback that consists in the consideration of the closest point P. Indeed, if the system is located the centre of the circle defined by the path-curvature present on the closest point, the guidance definition becomes singular and the ψ_c is no more uniquely defined. This singularity implies a restriction to the domain of validity of the derived control expression, inducing a highly-conservative initial condition $y_1(t=0) < c_{c,\max}^{-1}$, where $c_{c,\max}$ denotes the maximum curvature of the path. This restriction impedes the global nature of guaranteed performance requirement. Nevertheless, this solution stated a theoretical framework that allows for combined guidance / control design process, that will be used in the sequel.

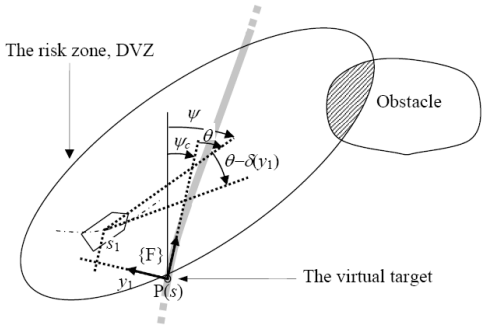

Fig. 6. problem pose for the virtual target principle and the DVZ principle.

4.4 Virtual target vehicle

An alternative to this problem has been originally proposed in (Soetanto *et al.*, 2003 and Lapierre[b] *et al.*, 2006) for an application to wheeled vehicle, extended to marine systems in (Lapierre[a] and Soetanto*, 2006). It consists in the development of the kinematic model of the vehicle in terms of a *Serret–Frenet* frame {*F*} that moves along the path; {*F*} plays the role of the body axis of a Virtual Target Vehicle that should be tracked by the 'real vehicle'. Using this set-up, the cross tracking distance y_1 and the angle $\theta - \delta(y_1)$ become the coordinates of the error space where the control problem is formulated and solved. A *Frenet* frame {*F*} that moves along the path to be followed is used with a significant difference with the previously described nonlinear approach guidance solution: *the Frenet frame is not attached to the point on the path that is closest to the vehicle*. Instead, the origin of {*F*} along the path is made to evolve according to a conveniently defined function of time, effectively yielding an extra controller design parameter $\dot{s}$: where s denotes the curvilinear abscissa of the point P, on the path, thus capturing the evolution of the virtual target along the path (cf. Fig. 6). The consequence is the apparition of another variable s_1, and the control objective is to simultaneously reduce s_1, y_1 and $\theta - \delta(y_1)$ to zero. This seemingly simple procedure allows lifting the stringent initial condition constraint $y_1(t=0) < c_{c,\max}^{-1}$, that arise with the path following controller described in (Samson & Ait-Abderrahim, 1991). The virtual target control law will be derived during the control design, allowing for a solution that exhibits global guaranteed performances.

4.5 Merging other requirements

The previous solutions allow for guiding a marine vehicle toward a desired path. The problem of merging these guidance laws with other requirements, related to obstacle avoidance, environmental effects, optimal route planning, etc. is a difficult subject. Different strategies are proposed, in connection with the criticity of the requirement. For example, the occurrence of an obstacle must induce a rapid reaction, while information about a bad weather present on the current route will imply a path replanning without requiring a reflexive action. Nevertheless, the increasing computing power makes conceivable an obstacle avoidance based on path replanning, so far the obstacle is detected early-enough. The path replanning strategy requires the system to design a safe path between detected obstacles and excluded zones that warrants the vehicle to safely reach the desired goal. The proposed methods are generally classified in two categories: i) Graph Method and ii) Potential Methods. The graph methods are decomposed in two steps: i) the graph construction, allowing investigating all the possible paths and ii) the choice of the optimal path, in concurrently evaluating each of the solution performance (Latombe, 1991). The potential method is based on the space decomposition in terms of fictive potentials. An obstacle or an excluded region will induce a repulsive potential while an attractive potential will be placed onto the goal location. Then searching for the lines of minimum potential allows for planning the possible paths. Analyse of their performances in terms of energy consumption or risks, allow extracting the optimal solution (Barraquand *et al.*, 1992). Nevertheless, these methods do not guarantee the absence of local minima, and the selected path may drive the robot at an undesired impasse (Koditschek 1987). In (Louste & Liégeois, 1998), the authors propose a method based on the *Navier-Stokes* equations of incompressible fluid, undergoing a difference of pressure between the origin and the goal. As the water will always find a way to leak (if possible) form a pressurized confined environment, the analysis of a simulated flow, extracting the routes of maximum fluid particles velocity, allows for finding a global route that travels between obstacles and reach the goal without encountering local minima. Under the assumption that an accurate map of the environment is available; it designs a global solution that guarantees the system to reach the goal, if this solution exists. The problem of coupling this solution with the kinematics requirements of the vehicle is still unsolved. Nevertheless, the simulation of the fluid flow induces heavy computational burden that disqualify this solution in a real time context.

4.6 Reactive obstacle avoidance

A reactive obstacle avoidance strategy will be preferred. This solution is using the Deformable Virtual zone (DVZ, Zapata *et al.*, 2004) principle where a kinematic-dependant potential is attached onto the system, in opposition to the classic potential methods where the map is potentially-active. The idea is to define around the robot a risk zone, the ZVD, in which any obstacle penetration induces a repulsive reaction. The shape of the ZVD is based on an arbitrary choice (generally elliptic), whose parameters are governed by the vehicle kinematics and state evolution. Since the ZVD is attached to the vehicle, both are sharing the same non-holonomic, or underactuated, constraints. The obstacle intrusion is quantified as the area of the penetration (I), cf. Fig. 6. Tedious but straightforward computation yields the jacobian relation between the vehicle velocities (u and r, for unicycle-type robot, $\mathbf{v}$ for marine vehicle) and I. The control design framework is then well posed, and a combined (guidance / obstacle-avoidance / control) design process is possible, in order to seek for solutions that exhibits global guaranteed performances, as detailed in (Lapierre[a] *et al.**, 2006).

The virtual target principle needs to be deeper investigated. An interesting extension is to attribute to the virtual target another extra degree of freedom, y_s. This could allow the point P to leave the path laterally, and design a virtual target control in order to fuse the all the requirements on this runner. Moreover, an adjustment of the s_1 variable will allow for using a second virtual target as a *scout* in order to provide a prediction, compatible with the control theoretical framework.

4.7 Deformable constellation

The consideration of the guidance problem in a multi-vehicles context is an exciting question, where the presence of obstacle in the immediate vicinity of the vehicles is omnipresent. A vehicle deviating from its nominal path may imply a reaction on the entire flotilla members, in order to keep the cohesion on the formation and insure a smooth return to a nominal situation. The principle of the Deformable Constellation, introduced in (Jouvencel *et al.*, 2001), allows for fusing different criteria, related to communication, minimal distance keeping and mission objectives (optimizing the acoustic coverage of the seabed, for example), and attribute to each member the appropriate individual guidance and control instructions. The theoretical framework of this solution needs to be clarified in order to extend its application and evaluate the guaranteed performances of this solution. Based on an extension of the Virtually Deformable zone, this solution allows conceiving the creation of an effective collaborative space, for which the objective of the navigation systems of all the members is to complete the knowledge. In this scope, the constellation guidance is not any more defined around an arbitrary formation, but governed by the obligation of particular measurements, prioritized in function of their necessity. This guidance problem of a flotilla in order to optimize the collaborative acquisition of a desired measurement is a hot topic of research.

5. Control

The Control System generates actuator signals to drive the actual velocity and attitude of the vehicle to the value commanded by the Guidance system.

The control problem is different in function of the system actuation and the type of mission the robot is tasked with. The actuation effects have been considered during the modelling process. While the Navigation system is providing an estimation of the necessary variables, the goal of the guidance system is to take into account the system holonomic property and the type of missions (pose stabilisation / long range routing), in order to cast the control problem under the form of desired values $\boldsymbol{\eta}_d$ and $\boldsymbol{\nu}_d$ to be tracked by $\boldsymbol{\eta}$ and $\boldsymbol{\nu}$, thanks to the control system.

5.1 Hovering

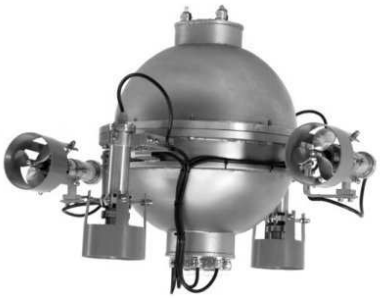

Fig. 7. The URIS ROV, Univerity of Girona, Spain.

The operating conditions allow for hydrodynamic model simplifications, and a pose-stabilisation problem implies small velocities that greatly reduce the model complexity. Moreover, vehicles designed for hovering are generally iso-actuated, or fully-actuated in the horizontal-plane and in heave (immersion), while the roll and pitch dynamics are passively stable (see, for instance the URIS ROV, Fig. 7). Then, hovering controller for ROVs are generally based on a linearization of the model of Equation (3), resulting in conventional PD or PID control laws (Whitcomb*, 2000). The navigation system, coupled with vision or acoustic devices provide a precise estimation of the vehicle pose, using for example the complentary filter depicted in Fig. 4 that fuses acceleration measurements with the vision system data, or the solution proposed in (Perrier, 2005) fusing Loch Doppler system velocities with dynamics features extracted form the video images.
Pose-stabilisation is an adequate situation to meet the linearizing condition requirements: i) small roll (ϕ) and pitch (θ) angles, ii) neutrally buoyant vehicle ($W = B$ and $\mathbf{r}_g = \mathbf{r}_b$) and iii) small velocities ($\mathbf{v}$). Considering these approximations and expressing the system model, Equation (3) in the *Vessel Parallel Coordinate System* {P} (a coordinate system fixed to the vessel with axes parallel to the Earth-fixed frame) allows for writing the system as the disturbed *Mass-Spring-Damper* system expressed in Equation (7).

$$\mathbf{M} \cdot \dot{\boldsymbol{\nu}} + \mathbf{D} \cdot \boldsymbol{\nu} + \mathbf{K} \cdot \boldsymbol{\eta}_P = \boldsymbol{\tau}_{PID} + \mathbf{w} \tag{7}$$

Where $\mathbf{M}$, $\mathbf{D}$ and $\mathbf{K}$ are constant matrices and $\boldsymbol{\eta}_P$ is $\boldsymbol{\eta}$ expressed in {P}. Classic methods for loop shaping allows for computing the appropriate values of the classic PID gains that results in the controlled forces and torques $\boldsymbol{\tau}_{PID}$. Nevertheless, a classic PD controller is reacting to the detection of a positioning error, and as a consequence, exhibits poor reactivity. The adjunction of the integral term, resulting in a PID controller, is improving this situation in implicitly considering a slow-varying external disturbance. Nevertheless, the low-dynamics integral action cannot provide the desired robust-stabilisation in a highly-disturbed environment. An interesting solution, called *Acceleration Feedback*, proposes to add an external control of the acceleration, $\boldsymbol{\tau}_{AF} = \mathbf{K}_{AF} \cdot \dot{\boldsymbol{\nu}}$, in order to consider 'as soon as possible' the occurrence of a disturbing action $\mathbf{w}$ on the system, where $\mathbf{K}_{AF}$ is a positive diagonal gain matrix, resulting in the following closed loop expression.

$$\mathbf{M} \cdot \dot{\boldsymbol{\nu}} + \mathbf{D} \cdot \boldsymbol{\nu} + \mathbf{K} \cdot \boldsymbol{\eta}_P = \boldsymbol{\tau}_{PID} + \boldsymbol{\tau}_{AF} + \mathbf{w}$$

Equivalently, and with some notation abuse,

$$\dot{\boldsymbol{\nu}} + \frac{\mathbf{D}}{\mathbf{M} + \mathbf{K}_{AF}} \cdot \boldsymbol{\nu} + \frac{\mathbf{K}}{\mathbf{M} + \mathbf{K}_{AF}} \cdot \boldsymbol{\eta}_P = \frac{\mathbf{1}}{\mathbf{M} + \mathbf{K}_{AF}} \boldsymbol{\tau}_{PID} + \frac{\mathbf{1}}{\mathbf{M} + \mathbf{K}_{AF}} \mathbf{w}$$

From this expression, it is noticed that besides increasing the mass from $\mathbf{M}$ to $\mathbf{M} + \mathbf{K}_{AF}$, acceleration feedback also reduces the gain in front of the disturbance $\mathbf{w}$ from $\mathbf{1}/\mathbf{M}$ to $\mathbf{1}/(\mathbf{M} + \mathbf{K}_{AF})$. Hence, the system is expected to be less sensitive to an external disturbance $\mathbf{w}$ if acceleration feedback is applied. This design can be further improved by introducing a frequency dependant acceleration feedback gain $\boldsymbol{\tau}_{AF} = \mathbf{H}_{AF}(s) \cdot \dot{\boldsymbol{\nu}}$, tuned according to the application. For instance, a low-pass filter gain will reduce the effects of high frequency disturbance components, while a notch structure can be used to remove 1st-order wave-induced disturbances (Sagatun *et al.*, 2001 and Fossen, 2002). Nevertheless, accelerometers are highly sensitive devices, which provide a high-rate measurement of the accelerations that the system is undergoing. As a consequence these raw measurements are noisy, and the acceleration feedback loop is efficient in the presence of important external

disturbances, guaranteeing the significance of the acceleration estimation, despite the measurement noise.

5.2 Manipulation

Recall that a precise dynamic positioning is of major importance for hovering control, especially if a manipulation has to be performed. Then, the manipulator and umbilical effects have to be explicitly considered. Moreover, as the simple presence of an umbilical link induces a dynamic effect on the vehicle, the manipulator that moves in a free space, without being in contact with a static immerged structure, generates also a coupling effect. This coupling effect is due to the hydrodynamic forces that react to the arm movement. A first approach is to consider the complete system (vehicle + manipulator), resulting in an hyper-redundant model expressing the dynamics of the end-effector in function of the actuation. Despite the linearization simplifications, the model remains complex and the control design is difficult and the performances are highly related to the accuracy of the model identification. Computed torque technique, (Gonzalez, 2004), allows for estimating the coupling effect on the link between the vehicle and the manipulator. Then the pose-stabilisation problem of the platform and the generation of the manipulator movement control are decoupled. Same approach can be used in order to compensate for the umbilical effect, meaning that a precise model of the hydrodynamical forces undergone by the cable is available. This is a difficult task since the umbilical cable is subject to disturbances along its entire length and the modelling requires having a precise knowledge of the currents and wave characteristics. An alternative, exposed in (Lapierre, 1999), proposes to use a force sensor placed on the link between the manipulator and the platform, in order to have a permanent measurement of the coupling. This coupling measurement, denoted $\mathbf{F}^{veh/man}$, is used to feed an external force control loop that corrects the position control of the vehicle (cf. Fig. 8).

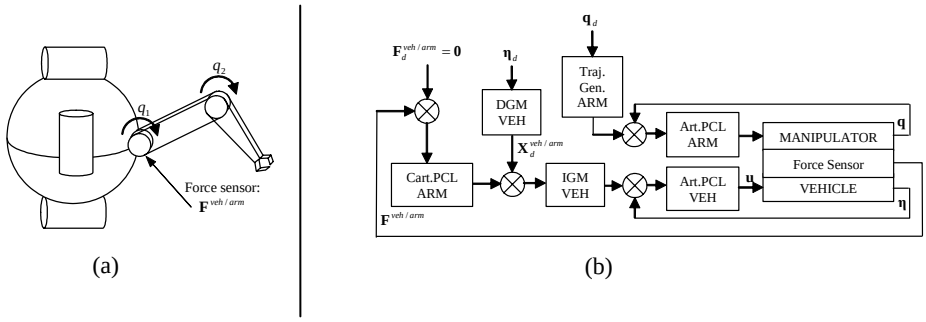

Fig. 8. problem pose and hybrid Position/Force external control structure.

Notice that the use of a single force control loop results in a reactive 'blind' system that exhibits a position steady-state error, while a single position control loop slowly, but precisely, correct the position error. Hence, the simultaneous control of the platform position and the coupling effect combines both the advantages of the force control reactivity and the precise steady control of the position. The manipulation generally consists in applying a desired force on an immerged structure on which an appropriate tool is performing the operation (drilling…). In this case, the coupling forces and torques present on the link between the manipulator and the platform is also due to the environment reaction to the operation. A steady state analysis underlines the necessity for the platform to apply the end-effector desired force on the coupling articulation. Nevertheless, since the

system is in contact with the environment, the coupling dynamics depends on the environment characteristics, generally modelled as a mass-spring-damper, and the thrusters' dynamics mounted on the vehicle. The solution proposed in (Lapierre, 1999) consists in a gain adaptation of the platform and of the manipulator controllers in order to combine the dynamics of both subsystems. Then, the low response of the platform is compensated by the high reactivity of the manipulator. This allows for performing free-floating moving manipulation, as required, for instance, for structure-cleaning applications.
Recent experimentations on the *ALIVE* vehicle[1] have demonstrated the feasibility of a simple underwater manipulation via an acoustic link, removing the umbilical cable necessity, and its drawbacks. The poor-rate acoustic communication does not allow real-time teleoperation, since real-time images transmission is impossible. Then, the teleoperation loop has to explicitly consider varying delays that greatly complicate the problem. A solution to this problem is detailed in (Fraisse *et al.**, 2003), and basically proposes to slow-down the manipulator time-response, in order to adapt the delicate force application to the erratic incoming of the reference, provided by the operator. The target approach phase requires the *Intervention AUV* (IAUV) to navigate over a relatively long distance, and it has to exhibit the quality of an AUV system. Indeed, the inefficiency of side thrusters during a high-velocity forward movement leads to consider the IAUV system as underactuated. Notice that a controller designed for path-following cannot naturally deal with station keeping, for underactuated system. This limitation has been clearly stated in (Brocket*, 1983), and can be intuitively understood as the impossibility for a nonholonomic system to uniformly reduce the distance to a desired location, without requiring a manoeuvre that will temporarily drives the vehicle away from the target. Moreover, in presence of ocean current, the uncontrolled sway dynamics (case of the underactuated system) impedes the pose-stabilisation with a desired heading angle. Indeed, the single solution is for the underactuated vehicle to face the current. As a consequence, IAUV systems are fully-actuated, but can efficiently manage the actuation at low velocity. The first solution consists in designing two controllers and switching between them when a transition between path-following and station keeping occurs. The stability of the transition and of both controllers can be warranted by relying on switching system theory (Hespanha *et al.*, 1999). The second solution consists in designing the path-following algorithm in such a way that it continuously degenerates in a point-stabilisation algorithm, smoothly adding the control of the side-thrusters, as the forward velocity is decreasing, retrieving the holonomic characteristic of the system (Labbe *et al.*, 2004). Notice that the powerful stern thrusters are not suited for fine control of the displacement. Then, these vehicles are equipped with added fine dynamic-positioning thrusters that lead to consider the system as over-actuated during the transition phase. The control of this transition implies to consider sequentially an uderactuated system, an over-actuated system, and finally an iso-actuated system. This specificity in the control of an IAUV system is a current topic of research.

5.3 Long-range routing

Control design for underactuated marine vehicles (AUVs, ASCs) has been an active field of research since the first autopilot was constructed by *E. Sperry* in 1911 (Fossen, 2002). Basically, it was designed to be a help for ship pilots in the heading control, while the forward movement was tuned according to a reasonable motor regime. Providing an accurate yaw angle measurement, classic PID controller allows for driving any conventional ship to a predefined list of set points.

[1] http://www.ifremer.fr/flotte/coop_europeenne/essais.htm and cf. Figure 9 in the paper *Underwater Robots Part I : current systems and problem pose.*

Enriching the navigation system with GPS measurements extends the application of this strategy to way-point routing and LOS guidance technique. Nevertheless, this seemingly-simple control scheme hides a complex problem in the gain tuning, for who requires the system to exhibit guaranteed performances, that is bounding the cross-tracking error along the entire route.

Linear Quadratic technique allows for designing a controller for the linearized system, which minimizes a performance index based on the error and time-response specifications (Naeem *et al.*, 2003 and Brian *et al.*, 1989). The linearization process of the model of a vessel in cruising condition assumes, upon the relevant conditions previously listed in the station-keeping case, i) a constant forward velocity ($u = u_d$) and ii) a small turning rate ($\dot{\boldsymbol{\eta}}_{\mathbf{P}} \approx \mathbf{v}$). This results in the state-space *linear time invariant* model:

$$\begin{aligned} \dot{\mathbf{x}} &= \mathbf{A} \cdot \mathbf{x} + \mathbf{B} \cdot \mathbf{u} + \mathbf{E} \cdot \mathbf{w} + \mathbf{F} \cdot \mathbf{v}_0 \\ \mathbf{y} &= \mathbf{C} \cdot \mathbf{x} \end{aligned} \tag{8}$$

where $\mathbf{x} = \left[\boldsymbol{\eta}_{\mathbf{P}}{}^{\mathrm{T}} \quad (\mathbf{v} - \mathbf{v}_0)^{\mathrm{T}} \right]^{\mathrm{T}}$, $\mathbf{v}_0 = [u_d \quad 0 \quad 0 \quad 0 \quad 0 \quad 0]^{\mathrm{T}}$,u=r. The expression of the 12×12 matrix $\mathbf{A}$, the 6x12 matrix $\mathbf{C}$ and the 12x6 matrices $\mathbf{B}$, $\mathbf{E}$ and $\mathbf{F}$ can be found in (Fossen, 2002). The control objective is to design a linear quadratic optimal controller that tracks, over a horizon T, the desired output $\mathbf{y_d}$ while minimizing:

$$J = \min_{\mathbf{u}} \left\{ \frac{1}{2} \cdot \int_{t_0}^{T} \left(\mathbf{e}^{\mathrm{T}} \cdot \mathbf{Q} \cdot \mathbf{e} + \mathbf{u}^{\mathrm{T}} \cdot \mathbf{R} \cdot \mathbf{u} \right) \cdot dt \right\}$$

where $\mathbf{Q}$ and $\mathbf{R}$ are tracking error and control positive weighting matrices. It can be shown (Brian *et al.*, 1989) that the optimal control law is

$$\mathbf{u} = -\mathbf{R}^{-1} \cdot \mathbf{B}^{\mathrm{T}} \cdot \left[\mathbf{P} \cdot \mathbf{x} + \mathbf{h}_1 + \mathbf{h}_2 \right]$$

where $\mathbf{P}$ is a solution of the *Differential Riccati Equation*, and $\mathbf{h}_1$ and $\mathbf{h}_2$ originates from the system *Hamiltonian*, and can be computed according to (Brian *et al.*, 1989).

Another approach, called **Feedback Linearization**, proposes to algebraically transform a nonlinear system dynamics into a (fully or partly) linear one, so that linear control techniques can be applied. This differs form conventional linearization, as exposed before, in that feedback linearization is achieved by exact state transformations and feedback, rather than by linear approximations of the dynamics (Slotine, 1991). The control objective is to transform the vessel dynamics (3) into a linear system $\dot{\mathbf{v}} = \mathbf{a}^{\mathbf{b}}$, where $\mathbf{a}^{\mathbf{b}}$ can be interpreted as a body-fixed commanded acceleration vector. Considering the nonlinear model of Equation (3), the nonlinearities of the controlled system can be cancelled out by simply selecting the control law as:

$$\boldsymbol{\tau}_{Feed.Lin.} = \mathbf{M}(\boldsymbol{\eta}) \cdot \mathbf{a}^{\mathbf{b}} + \mathbf{C}(\mathbf{v}) \cdot \mathbf{v} + \mathbf{D}(\mathbf{v}) \cdot \mathbf{v} + \mathbf{G}(\boldsymbol{\eta})$$

Notice that the injection of this control expression in the nonlinear model of Equation (3) provides the desired closed loop dynamic $\dot{\mathbf{v}} = \mathbf{a}^{\mathbf{b}}$. The commanded acceleration vector $\mathbf{a}^{\mathbf{b}}$ can be chosen by pole placement or linear quadratic optimal control theory, a described previously. The pole placement principle allows for selecting the system poles in order to specify the desired control bandwidth. Let $\boldsymbol{\Lambda} = \mathrm{diag}\{\lambda_1, \lambda_2, ..., \lambda_6\}$ be the positive diagonal

matrices of the desired poles λ_i. Let $\mathbf{v}_d$ denote the desired linear and angular velocity vector, and $\tilde{\mathbf{v}} = \mathbf{v} - \mathbf{v}_d$ the velocity tracking error. Then the commanded acceleration vector can be chosen as a PI-controller with acceleration feedforward:

$$\mathbf{a}^{\mathbf{b}} = \dot{\mathbf{v}}_d - \mathbf{K}_p \cdot \tilde{\mathbf{v}} - \mathbf{K}_i \cdot \int_0^t \tilde{\mathbf{v}}(\tau) \cdot d\tau$$

Choosing the gain matrices as $\mathbf{K}_p = 2 \cdot \mathbf{\Lambda}$ and $\mathbf{K}_i = \mathbf{\Lambda}^2$, as proposed in (Fossen, 2002), yields a second order error dynamics for which each degrees of freedom poles are in $s = -\lambda_i$ $(i = 1,...n)$, thus guaranteeing the system stability.

In (Silvestre *et al*., 2002), the authors propose an elegant method, called **Gain-Scheduling**, where a family of linear controllers are computed according to linearizing trajectories. This work is based on the fact that the linearization of the system dynamics about trimming-trajectory (helices parameterized by the vehicle's linear speed, yaw rate and side-sleeping angle) results in a linear time-invariant plant. Then, considering a global trajectory consisting of the piecewise union of trimming trajectories, the problem is solved by computing a family of linear controllers for the linearized plants at each operating point. Interpolating between these controllers guarantees adequate local performance for all the linearized plants. The controllers design can then be based on classic linear control theory.

Nevertheless, these issues cannot address the problem of global stability and performances. Moreover, the reader has noticed that these methods imply that the model parameters are exactly known. In Feedback Linearization technique, a parameter misestimation will produce a bad cancellation of the model nonlinearities, and neglect a part of the system dynamics that is assumed to be poorly excited. This assumption induces conservative conditions on the domain of validity of the proposed solution, thus greatly reducing the expected performances, which in turn, cannot be globally guaranteed.

The **Sliding Mode Control** methodology, originally introduced in 1960 by A. Filipov, and clearly stated in (Slotine, 1991), is a solution to deal with model uncertainty. Intuitively, it is based on the remark that it is much easier to control 1st-order systems, being nonlinear or uncertain, than it is to control general n^{th}-order systems. Accordingly, a notational simplification is introduced, which allows n^{th}-order problems to be replaced by equivalent 1st-order problem. It is then easy to show that, for the transformed problems, 'perfect' performance can in principle be achieved in the presence of arbitrary parameters accuracy. Such performance, however, is obtained at the price of extremely high control activity. The basic principles are presented in the sequel. Consider the nonlinear dynamic model of Equation (3), rewritten as:

$$\ddot{\boldsymbol{\eta}}_P = \mathbf{F}\left(\dot{\boldsymbol{\eta}}_P, \boldsymbol{\eta}_P\right) + \mathbf{H}\left(\boldsymbol{\eta}_P\right) \cdot \mathbf{u}$$

where $\boldsymbol{\eta}_P$ is $\boldsymbol{\eta}$ expressed in *Vessel Parallel Coordinate system* {P}, as defined previously. $\mathbf{F}$ and $\mathbf{H}$ are straightforward-computable nonlinear matrices expressed from Equation (3), that are not exactly known, and $\hat{\mathbf{F}}$ and $\hat{\mathbf{H}}$ are their estimation, respectively. A necessary assumption is that the extent of the precision of $\mathbf{F}$ is upper-bounded by a known function $\bar{\mathbf{F}}(\dot{\boldsymbol{\eta}}_\mathbf{P}, \boldsymbol{\eta}_\mathbf{P})$, that is $\left|\hat{\mathbf{F}} - \mathbf{F}\right| \le \bar{\mathbf{F}}$. Similarly, the input matrix $\mathbf{H}$ is not exactly known, but bounded and of known sign. The control objective is to get the state $\boldsymbol{\eta}_P$ to track a desired reference $\boldsymbol{\eta}_{P,d}$, in the presence of model imprecision on $\mathbf{F}$ and $\mathbf{H}$. For simplification reasons, we consider in the following that the $\mathbf{H}$ matrix is perfectly known. For a detailed description of a complete study case, please refer to (Slotine,

1991). Let $\tilde{\boldsymbol{\eta}}_p = \boldsymbol{\eta}_p - \boldsymbol{\eta}_{p,d}$ be the tracking error vector. Let **s** be a vector of a weighted sum of the position and the velocity error, defining the *sliding surface* $S(t)$.

$$\mathbf{s} = \dot{\tilde{\boldsymbol{\eta}}}_P + \boldsymbol{\lambda}_1 \cdot \tilde{\boldsymbol{\eta}}_P$$

where $\boldsymbol{\lambda}_1$ is a diagonal matrix composed with strictly positive gains. With this framework, the problem of tracking $\boldsymbol{\eta}_p \equiv \boldsymbol{\eta}_{p;d}$ is equivalent of remaining on the surface *S(t)* , for all *t* ; indeed $\mathbf{s}(t) \equiv 0$ represents a 1st-order linear differential equation whose unique solution is $\tilde{\boldsymbol{\eta}}_p \equiv 0$, given initial condition $\boldsymbol{\eta}_p(0) = \boldsymbol{\eta}_{p,d}(0)$. The problem of keeping the scalar components of **s** at zero can now be achieved by choosing the control law **u** such that, outside *S(t)*:

$$\frac{1}{2}\frac{d}{dt}\mathbf{s}^2 \le -\boldsymbol{\lambda}_2{}^{\mathrm{T}} \cdot |\mathbf{s}| \tag{9}$$

where $\boldsymbol{\lambda}_2$ is a vector composed with strictly positive gains, $\mathbf{s}^2$ is the vector composed with the squared components of **s** and $|\mathbf{s}|$ is the vector composed with the absolute values of the component of **s**. Essentially, the previous expression is called the *sliding condition,* and states that the square 'distance' to the surface, as measured by $\mathbf{s}^2$, decreases along all trajectories, thus making the surface *S*(*t*) an *invariant set*. The design of **u** is done in two steps. The first part consists in controlling the system dynamics onto the surface *S*(*t*), expressed as $\dot{\mathbf{s}} = 0$. Assuming that **H** is invertible, solving formally this previous equation for the control input, provides a first expression for **u** called the *equivalent control*, $\mathbf{u}_{eq}$, which can be interpreted as the continuous control law that would maintain $\dot{\mathbf{s}} = 0$ if the dynamic were exactly known.

$$\mathbf{u}_{eq} = \mathbf{H}^{-1} \cdot \left[-\hat{\mathbf{F}} + \ddot{\boldsymbol{\eta}}_{\mathbf{d}} - \boldsymbol{\lambda}_1{}^{\mathrm{T}} \cdot \dot{\tilde{\boldsymbol{\eta}}} \right]$$

The second step tackles the problem of satisfying the switching condition, Equation (9), despite uncertainty on the dynamics **F** (for simplicity the input matrix **H** is assumed to be perfectly known), and consists in adding to $\mathbf{u}_{eq}$ a term discontinuous across the surface

$$\mathbf{s} = 0 :$$
$$\mathbf{u} = \mathbf{u}_{eq} - \mathbf{H}^{-1} \cdot \boldsymbol{\lambda}_3 \cdot \mathbf{sign}(\mathbf{s})$$

where $\boldsymbol{\lambda}_3$ is a matrix composed with strictly positive functions $\lambda_{3,i}$, and **sign(s)** denotes the vector where the i^{th} element equals to +1 is $s_i > 0$, or -1 if $s_i < 0$. By choosing $\lambda_{3,i} = \lambda_{3,i}(\dot{\boldsymbol{\eta}}_P, \boldsymbol{\eta}_P)$ to be 'large enough', we can now guarantee that the sliding condition (9) is satisfied. Indeed, we obtain the expression:

$$\frac{1}{2}\frac{d}{dt}\mathbf{s}^2 = \left[\mathbf{F} - \hat{\mathbf{F}}\right] \cdot \mathbf{s} - \boldsymbol{\lambda}_3 \cdot |\mathbf{s}|$$

which is a negative definite vectorial expression if the functions $\lambda_{3,i}(\dot{\boldsymbol{\eta}}_P, \boldsymbol{\eta}_P)$ are chosen according to the choice of:

$$\boldsymbol{\lambda}_3 = \hat{\mathbf{F}}(\dot{\boldsymbol{\eta}}_{\mathbf{P}}, \boldsymbol{\eta}_{\mathbf{P}}) + \boldsymbol{\varepsilon}(s)$$

where $\boldsymbol{\varepsilon}(s)$ is a positive margin vector. This implies that the system will effectively converge towards the sliding surface, on which the trajectories are all converging to the origin. The consideration of a misestimation in the input matrix **H**, brings into the choice of the $\lambda_{3,i}$ the guaranteed upper and lower bounds $\mathbf{H}^{max}$ and $\mathbf{H}^{min}$ on the uncertainty of **H**, (Slotine, 1991).
This control technique has been applied in various systems, and an application to the Taipan 1 AUV is detailed in (Vaganay *et al*., 1998), where the authors uses the control robustness to compensate for the uncertainty of a linear equivalent controller $\mathbf{u}_{eq}$. The main drawback of this method is the extremely high control activity that generates the switching part of the control scheme, induced by excited unmodelled dynamics. Moreover, bounds on the components of **s** can be directly translated into bounds on the tracking error vector $\tilde{\boldsymbol{\eta}}_{\mathbf{P}}$, and therefore the components of s represent a true measure of tracking performance.
Nonlinear control design, based on *Lyapunov* theory and *Backstepping* technique, allows for considering the full nonlinear model of the system and the model uncertainty in order to guarantee asymptotic performances of the controlled system. The problem and the model are decoupled according to the three planes of evolution, vertical, horizontal and transverse planes, where the control objectives are *path-following*, *diving control* and *roll compensation*. We illustrate in the following an application of this solution to the vehicle Taipan 2[2]). The three simplified nonlinear models are written as:

- Path-following in the Horizontal Plane

The dynamic horizontal model is extracted from the model of Equation (3), as:

$$\begin{aligned} F_u &= m_u \cdot \dot{u} + d_u \\ 0 &= m_v \cdot \dot{v} + m_{ur} \cdot u \cdot r + d_v \\ \Gamma_r &= m_r \cdot \dot{r} + m_{pq} \cdot p \cdot q + d_r \end{aligned} \tag{10}$$

where F_u is the surge force induced by stern propellers and Γ_r is the controlled torque induced by rudder or differential action of stern thrusters, $m_u = m - X_{\dot{u}}$ is the system mass including inertial (m) and added ($X_{\dot{u}}$) masses along the surge direction, $m_v = m - Y_{\dot{v}}$ is the system mass in the sway direction and $m_r = I_{zz} - N_{\dot{r}}$ is the moment of inertia of the system around the z axis, including the intrinsic moment of inertia (I_{zz}) and the moment of inertia induced by added mass ($N_{\dot{r}}$). $m_{ur} = m - Y_{ur}$ and $m_{pq} = I_{yy}$ are cross-coupling velocity terms and d_u , d_v and d_r are hydrodynamic damping and restoring terms, whose expressions can be found in (Lapierre[c] et al., 2006).X, Y, and N are the hydrodynamic derivatives composing the matrices of the model of Equation (3). From the control expression , the relevant parameters are m_u , m_r , m_r , m_{ur} , m_{pq} , d_u , d_v and d_r , and constitute the parameter vector **p**.
The kinematic model is reduced to the rotation matrix **R**, expressing the following relations:

$$\begin{aligned} \dot{x} &= u \cdot \cos(\psi) - v \cdot \sin(\psi) \\ \dot{y} &= u \sin(\psi) + v \cos(\psi) \\ \dot{\psi} &= r \end{aligned} \tag{11}$$

The chosen guidance system is based on the *virtual target vehicle* principles. As described before, this method requires parameterizing the desired path in function of a curvilinear abscissa s of a

[2] cf. Figure 10 in the paper *Underwater Robots Part I : current systems and problem pose.*

point P(*s*), moving along the path, and defining an approach angle δ as described in Equation (6). The coordinates of the point P are expressed as $[s_1 \quad y_1]^T$ in the body-frame {*B*}. Equipped with this formalism, the control objective can be expressed as follows:

Consider the AUV model with kinematic and dynamic equations given by (3) and (11), respectively. Given a path to be followed, a desired $u_d > u_{\min} > 0$ *for the surge speed u, and a set of reasonable estimation of the parameter set* $\hat{\mathbf{P}}$ *, derive feedback control laws for the force* F_u *, torque* Γ_r *, and rate of evolution* $\dot{s}$ *of the curvilinear abscissa s of the "virtual target" point P along the path so that* y_1 *,* s_1 *,* ψ *, and* $u - u_d$ *tend to zero asymptotically.*

This problem decomposed in three sub-objectives.

i Global Uniformly Asymptotic Convergence (GUAC) of the **kinematic level**.

Expressing the kinematic model in the body frame, and considering the total velocity of the system $v_t = \left(u^2 + v^2\right)^{1/2}$ and the *side-slip* angle $\beta = \arctan(v/u)$, yields:

$$\begin{aligned} \dot{s}_1 &= -s \cdot (1 - c_c \cdot y_1) + v_t \cdot \cos(\psi_t) \\ \dot{y}_1 &= -c_c \cdot \dot{s} \cdot s_1 + v_t \cdot \sin(\psi_t) \\ \dot{\psi}_t &= r + \dot{\beta} - c_c \cdot \dot{s} \end{aligned} \tag{12}$$

In the kinematic case, the control input is reduced to *r*, the yaw-rate, and *u* is assumed to be equal to u_d. Recall that the virtual target principle requires to define the approach angle $\delta(y_1)$, given in Equation (6), and that the guidance objective is to make the angle θ tracking $\delta(y_1)$. This sub-problem is solved in considering an appropriate *Lyapunov* candidate function $V_1 = \frac{1}{2} \cdot (\theta - \delta(y_1))^2$, and extract control *r* satisfying the condition that $V_1 \cdot \dot{V}_1 < 0$ if $\theta \neq \delta$. Then, verifying that $\ddot{V}_1$ is bounded complete the requirements of the application of the *Barbalat*'s lemma (Khalil, 2002) which allows proving that the sub-set defined as the system trajectories where the approach error is null, $\Omega_1 := [\theta - \delta(y_1) = 0]$ is *invariant*. Then, the analysis of a second Lyapunov candidate $V_2 = \frac{1}{2} \cdot \left(s_1^2 + y_1^2\right)$, restricted onto Ω_1, and the use of the *LaSalle*'s theorem (Khalil, 2002) show the implicit consecutive convergence of the system toward the path, if the system is autonomous, that is if the desired forward velocity u_d is time invariant. This is stated in the following proposition:

Consider the robot model (10) and (11) and let a desired approach angle be defined by Equation (6). Further assume that measurements of $[u \quad v]^T$ *are available from robot sensors and that a parameterization of the path is available such that: given s , the curvilinear abscissa of a point on the path, the variables* θ *,* y_1 *,* s_1 *and* $c_c(s)$ *are well-defined and computable, where* $c_c(s) = \frac{d\psi_c}{ds}$ *denotes the path curvature at s. Then the kinematic control law:*

$$\begin{cases} r = \dfrac{1}{1 - \dfrac{m_{ur}}{m_r} \cdot \cos^2\beta} \cdot \left(\dot{\delta} + \dfrac{u}{v_t^2} \cdot \dfrac{d_v}{m_v} - k_1 \cdot (\psi - \delta) + c_c(s) \cdot \dot{s} \right) \\ \dot{s} = v_t \cdot \cos\psi + k_2 \cdot s_1 \end{cases} \tag{13}$$

applied to a stern-dominant vehicle, drives θ, y_1 *and* s_1 *asymptotically to zero, with* k_1 *and* k_2 *2 arbitrary positive gains, and given the initial relative position* $[\theta, s_1, y_1]_{t=0}$. *That is, the kinematic model of the AUV is asymptotically and uniformly converging to the desired path.*

Notice the 'stern dominant' condition is required in order to insure that:

$$\frac{m_{ur}}{m_v} = \frac{m - Y_{ur}}{m - Y_{\dot{v}}} < 1$$

It is interesting to notice that this condition has been stated in (Lewis*, 1988), according to different consideration, and is related to the open-loop stability of the system, restricted to the horizontal plane.

ii. Global Uniformly Asymptotic Convergence (GUAC) of the **dynamic level**.

The above feedback control law applies to the kinematic model of the AUV only. However, using B*ackstepping* techniques (Krstić, 1995), this control law can be extended to deal with vehicle dynamics. In the kinematic design the total velocity $v_t(t)$ of the vehicle was left free, but implicitly dependent on a desired time-invariant profile u_d for surge speed $u(t)$. In the dynamic design the variable u will be brought explicitly into the picture and a control law will be derived so that $u_d - u(t)$ tends to zero. Notice also that the robot's angular speed r was assumed to be a control input. This assumption is lifted by taking into account the vehicle dynamics. The following result holds.

Consider the robot model (10) and (11), and the corresponding path following error model in (12). Let a desired approach angle be defined by Equation (6) and let the desired speed profile $u_d > u_{\min} > 0$. *Further assume that measurements of* $[u \quad v \quad r]^{\mathrm{T}}$ *are available from robot sensors and that a parameterization of the path is available such that: given s, the curvilinear abscissa of a point on the path, the variables* θ, y_1, s_1 *and* $c_c(s)$ *are well-defined and computable. Then the dynamic control law:*

$$\begin{cases} \Gamma_r = m_r \cdot \alpha_r - d_r \\ F_u = m_u \cdot (\dot{u}_d - k_4 (u - u_d) - d_u) \\ \dot{s} = v_t \cdot \cos\psi + k_2 \cdot s_1 \end{cases} \tag{14}$$

where

$$\alpha_r = \frac{f_{\alpha_r} - k_3 \cdot (r - r_d) - k_5 \cdot (\theta - \delta)}{1 - \frac{m_{ur}}{m_v} \cdot \cos^2 \beta}$$

$$f_{\alpha_r} = \ddot{\delta} - k_1 \cdot (\dot{\theta} - \dot{\delta}) + c_c \cdot \ddot{s} + g_c \cdot \dot{s} + \frac{\ddot{u} \cdot v}{v_t^2} + \frac{2 \cdot \dot{v}_t \cdot \dot{\beta}}{v_t} + \frac{u}{v_t^2} \cdot \left(\frac{m_{ur}}{m_v} \cdot \dot{u} \cdot r + \frac{\dot{d}_v}{m_v} \right)$$

$$r_d = \dot{\delta} - \dot{\beta} - k_1 \cdot (\theta - \delta) + c_c(s) \cdot \dot{s}$$

and k_i, *for* i=1,…5, *are arbitrary positive gains, and given the initial relative position* $[\theta, s_1, y_1]_{t=0}$, *drives the system dynamics in order for* θ, y_1 *and* s_1 *to asymptotically and uniformly converge to zero, assuming a perfect knowledge of* $\mathbf{p}$.

This solution is derived according to the consideration of the *Lyapunov* candidate function $V_3 = \frac{1}{2} \cdot (r - r_d)^2 + \frac{1}{2} \cdot (u - u_d)^2$, capturing the convergence properties of the system yaw rate to the kinematic reference r_d, which is a rewriting of the kinematic control solution previously exposed. Using same type of argument than used for the

kinematic case, it can be shown that this convergence requirement induces the dynamic model of the system to asymptotically and uniformly converge to the path. For a complete proof, please refer to (Lapierre[a] & Soetanto*, 2006) and (Lapierre[b]* *et al.*, 2003).

iii. **Robust** Global Uniformly Asymptotic Convergence (GUAC) of the **dynamic level**.

This section addresses the problem of robustness to parameters uncertainty. The previous control is modified to relax the constraint of having a precise estimation of the dynamic parameter vector **P**, by resorting to backstepping and Lyapunov-based techniques. Recall that the kinematic reference expression involves the estimation of the horizontal model dynamic parameters. Let $r^{\text{opt}}(\mathbf{P})$ be the kinematic control law computed with the exact dynamic parameters, as expressed in Equation (12), and let $\hat{r}_d(\hat{\mathbf{P}})$ be the evaluation of this control expression, considering the approximated value of the parameters. It is straightforward to show that the neglected dynamics $\tilde{\mathbf{P}}$, induces a non negative derivative of the V_1 *Lyapunov* candidate, $\dot{V}_1 = -k_1 \cdot (\theta - \delta)^2 + (\theta - \delta) \cdot \Delta r$, where $\Delta r = r^{\text{opt}} - \hat{r}_d$.

The design of the dynamic control is done as previously, considering the Lyapunov candidate $V_3 = \frac{1}{2} \cdot (r - \hat{r}_d)^2 + \frac{1}{2} \cdot (u - u_d)^2$. The resulting control is expanded in order to make explicitly appear the parameters, and results in the following affine expression:

$$\begin{cases} \Gamma_r = \sum_{i=1}^{7} p_i \cdot f_i \\ F_u = \sum_{i=8}^{11} p_i \cdot f_i \\ r_d = \dfrac{f_r + \sum_{j=1}^{2} q_i \cdot g_i - \dot{u} \cdot \dfrac{v}{v_t^2}}{1 - q_3 \cdot g_3} \end{cases} \tag{15}$$

where $p_i(\mathbf{P})$ and $q_j(\mathbf{P})$ ($i = 1,...,11$ and $j = 1,2,3$) express groups of the system dynamics parameters, and $f_i(\boldsymbol{\eta}, \boldsymbol{\nu})$, $g_j(\boldsymbol{\eta}, \boldsymbol{\nu})$ and $f_r(\boldsymbol{\eta}, \boldsymbol{\nu})$ are functions dependant on the system states. Let $\Delta p_i = p_i(\mathbf{P}) - \hat{p}_i(\hat{\mathbf{P}})$ and $\Delta q_j = q_j(\mathbf{P}) - \hat{q}_j(\hat{\mathbf{P}})$ be the estimation error in the evaluation of the parameters p_i, involved in the control previous control expression. The misestimation Δp_i induces $\dot{V}_3$ to be non negative-definite, as:

$$\dot{V}_3 = -k_3 \cdot (r - \hat{r}_d)^2 - k_4 \cdot (u - u_d)^2 + \Delta \dot{V}_3 ,$$

where

$$\Delta \dot{V}_3 = \sum_{i=1}^{7} (r - \hat{r}_d) \cdot \Delta p_i \cdot f_i + \sum_{i=8}^{11} (u - u_d) \cdot \Delta p_i \cdot f_i \cdot$$

Then the consideration of the *Lyapunov* candidate $V_4 = V_3 + \frac{1}{2} \cdot \sum_{i-1}^{11} \frac{\Delta p_i^{\,2}}{\lambda_i}$ leads to pose:

$$\begin{aligned}\dot{\hat{p}}_i &= -\lambda_i \cdot (r - \hat{r}_d) \cdot f_i, \text{ for } i = 1,...,7 \\ \dot{\hat{p}}_i &= -\lambda_i \cdot (u - u_d) \cdot f_i, \text{ for } i = 8,...,11\end{aligned} \tag{16}$$

in order to obtain $\dot{V}_4 \leq 0$. This is done implicitly using the fact that $\Delta\dot{p}_i = \dot{\hat{p}}_i$, since $p_i(\mathbf{P})$ is assumed to be static. This parameter adaptation is possible since the parameters p_i appear in an affine form in the control expression. Recall that the control (15) has been designed to drive the system toward the reference $\hat{r}_d$, whose expression involves an estimation of the some of the dynamical parameters. As a consequence, the control (15) with the adaptation scheme (16) drive asymptotically the system toward the non-exact kinematic reference $\hat{r}_d$. In order to recover the GUAC requirement, the parameters q_j need to be adapted. The adaptation design previously-used cannot be applied since the nonlinear form in which the parameter q_3 appears. Then, the robust scheme is developed relying on *switching system theory*, applied to control design, as stated in (Hespanha *et al.*, 1999). Concerning marine systems and our system of Equation (15), the robust scheme relies on the choice two different values q_j^{up} and q_j^{down}, guaranteed to overestimate and underestimate the real value q_j ($\Delta q_j^{up} > 0$ and $\Delta q_j^{down} < 0$), and use them according to:

$$\begin{aligned}q_j &= \begin{cases} q_j^{up} \text{ if } (\theta - \delta) \cdot g_j < 0 \\ q_j^{down} \text{ elsewhere} \end{cases} \\ q_3 &= \begin{cases} q_3^{up} \text{ if } (\theta - \delta) \cdot g_3 \cdot r < 0 \\ q_3^{down} \text{ elsewhere} \end{cases}\end{aligned} \tag{17}$$

Using the fact that $g_3 > 0$ and $1 - q_3 \cdot g_3 > 0$, it can be shown (Lapierre[b] & Soetanto, 2006), that the Lyapunov function $V_1 = (\theta - \delta)^2$, restricted to the invariant set $\Omega_r := [r - r_d = 0]$ has a following negative expression:

$$\dot{V}_1 = \frac{(\theta - \delta)}{1 - q_3 \cdot g_3} \cdot \left(\sum_{j=1}^{2} \Delta q_i \cdot g_i + \Delta q_3 \cdot g_3 \cdot r \right) \leq 0$$

At last, we can state the final proposition:

Consider the robot model (10) and (11), and the corresponding path following error model in (12). Let a desired approach angle be defined by Equation (delta) and let the desired speed profile $u_d > u_{\min} > 0$. *Further assume that measurements of* $[u \quad v \quad r]^T$ *are available from robot sensors and that a parameterization of the path is available such that: given s, the curvilinear abscissa of a point on the path, the variables* θ, y_1, s_1 *and* $c_c(s)$ *are well-defined and computable.*

Consider that a reasonable estimation of the model parameters **P**, *is used to compute the 11 initial values* $\hat{p}_i$ *and the 3 pairs* q_j^{up} *and* q_j^{down} *such that* $q_j^{downn} < q_j < q_j^{up}$. *Then the control law* (15), *with the adaptation scheme (16) and the switching scheme (17), and given the initial relative position* $[\theta, s_1, y_1]_{t=0}$, *solves the robust path-following problem.*

- Vertical plane

The dynamic vertical model is extracted from the model of Equation (3), as:

$$\begin{aligned} F_u &= m_u \cdot \dot{u} + d_u \\ F_w &= m_w \cdot \dot{w} + m_{uq} \cdot u \cdot q + d_w \\ \Gamma_q &= m_q \cdot \dot{q} + m_{pr} \cdot p \cdot r + d_q \end{aligned} \tag{18}$$

where F_u is the vertical force induced by the common action of the stern and bow control surfaces and Γ_q is the torque applied around the sway direction, induced by the differential action of the control surfaces. $m_w = m - Z_{\dot{w}}$ is the system mass including inertial (m) and added mass ($Z_{\dot{w}}$) along the heave direction and $m_q = I_{yy} - M_{\dot{q}}$ is the moment of inertia of the system around the y axis, including the intrinsic moment of inertia (I_{yy}) and the moment of inertia induced by added mass ($M_{\dot{q}}$). $m_{uq} = -m$ and $m_{pr} = -I_{zz}$ are cross-velocities coupling terms and d_w and d_q are hydrodynamic damping and restoring terms, whose expressions can be found in (Lapierre[c] *et al.*, 2006).*X*, *Z*, and *M* are the hydrodynamic derivatives composing the matrices of the model of Equation (3).

A similar strategy than exposed previously for the horizontal plane is used detailed in (Lapierre[c] et al., 2006). Nevertheless, considering an AUV with bow and stern control surfaces (case of the vehicles *Taipan 2*[3] and *Infante*, ISR, Lisbon Portugal), the system model is fully actuated, assuming a strictly positive forward velocity. Indeed, an AUV only carrying stern control surfaces (case of the vehicles *Remus* - Hydroid Inc., Cape Cod, MA, USA - and *Gavia* - Hafmynd, Reykjavic, Island) cannot be actuated along the *z* axis. Moreover, the UUV systems are generally positively buoyant, for safe recovery reason. This induces on the system a constant upward force, which requires to be compensated in pitching negatively. Then, such a system cannot insure a precise depth control with a null pitch angle. In opposition, a fully-actuated AUV in the diving-plane, is capable of changing depth with a constant (even null) pitch angle, and compensate the positive buoyancy during constant pitch and depth control. This makes these systems particularly well-suited for shallow-water or near-bottom applications, where a precise depth and pitch control is required. From the control point of view, the designer is facing an over-constrained problem, where two strategies exist for changing depth. This trade-off is solved at the guidance level in combining both strategies according to the system situation. An obstacle avoidance manoeuvre, or a change in the bottom profile, may induce a rapid reaction, and the pitch strategy will be preferred. On the other hand, a precise survey is requiring a null pitch angle, and a smooth evolution of the distance to the bottom can be compensated without modifying the system attitude. A solution to this problem is detailed in (Lapierre[c] et al., 2006). The adaptation design benefits from the fully-actuated nature of the system, and classic continuous method (in opposition to switching) works. Nevertheless, the work in (Lapierre & Jouvencel*, 2006) underlines a major drawback of the method. That is the evolution of the parameters estimate ($\dot{\hat{p}}_i$ in the horizontal case), is not guaranteed to be bounded in presence of sensor noise. Then, the authors propose to design a robust switching scheme (as done for the parameters $\hat{q}_j$ in the horizontal case) for all the system parameters. This leads to a discontinuous evolution of the control inputs, and the effect on the actuator activity has to be

[3] cf. Figure 10 in the paper *Underwater Robots Part I : current systems and problem pose.*

explicitly studied. Notice the analogy of this solution with the sliding-mode control design as exposed previously. This warrants further research on this topic.

- Transverse plane

$$0 = m_{\dot{v}} \cdot \dot{v} + m_{ur} \cdot u \cdot r + d_v$$
$$F_w = m_w \cdot \dot{w} + m_{uq} \cdot u \cdot q + d_w$$
$$\Gamma_p = m_p \cdot \dot{p} + d_p$$

where Γ_p is the torque applied around the surge direction, induced by the propeller rotation. $m_p = I_{xx} - K_{\dot{p}}$ is the moment of inertia of the system around the x axis, including the intrinsic moment of inertia (I_{xx}) and the moment of inertia induced by added mass ($K_{\dot{p}}$). d_p is the hydrodynamic damping and restoring term, whose expressions can be found in (Lapierre & Jouvencel*, 2006).

The control objective in the transverse plane is to keep the rolling angle ϕ as small as possible. Indeed, the decoupling condition is that $\phi \approx 0$. Considering the symmetrical shape of the system, the principal excitation of the rolling dynamics is due to the stern thrusters' activity, which for a given motor regime induces a rolling torque. This compensation is generally statically performed with static fins placed in the propeller flow.

5.4 Biological Inspired systems.

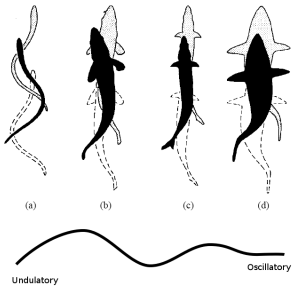

Fig. 9. Swimming movement from (a) anguiliform, through (b) sub-caranguiform and (c) caranguiform to (d) thunniform mode, from (Lindsey, 1978).

All type of vertebrate locomotion relies on some kind of rhythmic activity to move forward: undulations or peristaltic contractions of the body, and/or oscillations of fins, leg or wings. By rhythmically applying forces to the environment (ground, water or air), reaction forces are generated which move the body forward. This type of locomotion is in contrast to the most man-made machines which usually rely on few degrees of freedom (e.g. a limited number of powered wheels, propellers, or jet engines), and continuous, rather than rhythmic, actuation. From a technological point of view, animal locomotion is significantly more difficult to control than most wheeled or propelled machines. The oscillations of the multiple degrees of freedom need indeed to be well coordinated to generate efficient locomotion, (Ijspeert, 1995). These oscillations are produced by the system actuation, controlled to follow a desired body-shape deformation profile, called *locomotive gait*. The choice of the locomotive gait is a crucial question. In the case of an eel-like robot, this body-shape evolution is a propagating wave, adjusting the signal phase according to the joint situation located on each vertebra. Indeed, a

badly chosen gait will agitate the robot without guaranteeing that the maximum number of system elements (vertebrae) is involved in the thrust generation, loosing by the way the desired efficiency in terms of propulsion and manoeuvrability. Biologists have identified different types of gait in function of the animal, from undulatory to oscillatory movement (this study does not consider locomotion induced by fins movement), cf. Fig. 9.
Using *in vivo* observations, E. Tytell, in (Tytell, 2003) proposes a generic mathematical expression of the gait profile, expressing the lateral (y) position of the animal midline.

$$y(s_e) = A \cdot e^{\alpha \cdot (s_e / L - 1)} \cdot \sin\left(\frac{2/\pi}{\lambda} \cdot (s_e - V \cdot t) \right) \tag{19}$$

where s_e is the contour length along the midline starting at the head, A is the tail beat amplitude, α is the amplitude growth rate, L is the body length, λ is the body wave length, t is time and V the body wave speed. By this definition, a large α implies that amplitude is low near the head and increases rapidly near the tail. A smaller a implies more undulation anteriorly. This author proposes also an adaptation profile of the parameter a at a given speed.
From a robotics aspect, the motion control problem can be divided in three questions.

i. The system ability to produce a thrust according to a desired forward velocity. This question underlies three points.
   - The gait choice.
   - The control of the joint actuation in order to follow the previous reference.
   - The adaptation of the gait parameters according to the system situation.
ii. The control of the system heading according to a desired reference.
iii. The combination of both the previous solutions according to path following requirement.

The literature proposes some actuation gaits, directly controlling the inter-vertebrae actuation as a trajectory tracker. In (McIsaac & Ostrowski, 2002), the following actuation sinusoidal gait has been chosen.

$$\varphi_i(t) = A \cdot \sin(\omega \cdot t + (i-2) \cdot \varphi_s) + \varphi_{\text{off}} \tag{20}$$

where φ_i is the joint angle of the articulation i, t is the time, A maximum amplitude of the oscillation, ω is the wave frequency, φ_s is a constant phase difference between links, and φ_{off} is the parameters that acts on the system angular velocity. Clearly, this choice is a sub-expression of (19), with the difference that (20) expresses a temporal joints evolution, when (19) describes the body shape evolution. Indeed, despite the mathematical expression similarity, nothing guarantees that a perfect tracking of the joint reference (20) induces for the system to geometrically converge to the shape described in (19). Saintval, in (Saintval, 2002), proposes an optimal approach to find the best parameter's gait for a three-links robotic carangiform prototype. As underlined by G. Gillis (Gillis, 1998), natural eels are adapting the gait parameters in function of the forward speed. For examples, the analysis of the observations done by G. Gillis shows clearly that tailbeat frequency increases significantly with swimming speed. Moreover this relation tailbeat frequency / forward speed appears to be linear, this results is also observed by D. Webber *et al*, in (Webber *et al.*, 2001).
The work reported in (Lapierre & Jouvencel, 2005) and (Parodi *et al.*, 2006) started a study in order to design a closed loop control of the serial chained system (representing the eel) that adapts the gait profile in function of the system situation in order to increase performance. The starting point comes again from a biological inspiration, stating that fishes are using lateral line sensors to monitor the surrounding flow field for manoeuvring underwater, (Fan *et al.*, 2002). This pressure

sensors line allows fishes to locally control the fluid flow quality along their body. This observation gives a very interesting intuition on how closing the control loop in order to improve the system performance. The adopted methodology is following the 6 following points.

i. Designing an autonomous gait: literature proposes actuation gaits which are explicitly time-dependent. Moreover, the shape deformation is induced directly by a joint trajectory tracker. This is the classic problem of path following *versus* trajectory tracking. As shown for the case of nonholonomic wheeled robot [25] or underactuated marine craft, a path following controller achieve smoother convergence to a path, when compared to trajectory tracking control law, and the control signals are less pushed to saturation. Moreover, from a theoretical aspect, powerful mathematical tools are available for autonomous system, which are not usable in the case of non autonomous systems, (Lapierre & Jouvencel, 2005).
ii. Controlling the curvature profile: this allows for controlling effectively the body shape, instead of applying directly the actuation gait. The analogy with the gaits coming from biological observation is direct. Moreover, this method allow for closing the control loop on the system states, resulting in an efficient system regulation, (Lapierre & Jouvencel, 2005).
iii. Adapting the gait parameters in function of the system situation: the previous theoretical framework permits the design of an adaptive scheme, improving performance, (Parodi *et al.*, 2006).
iv. Coupling with path following requirement: the gait parameters are modified in order to guarantee the system to reach and follow a desired path, (Lapierre & Jouvencel, 2005).
v. Coupling with a local force control: this item concerns an active open issue. Notice that the previous solutions (autonomous or not) are closing the control loop on an arbitrary reference, resulting in a shape control without explicit connection with the fluid. The solution consists in combining the previous solution with a local force control requirement in order to adjust the previous gait and improve system performances.
vi. Designing a pure force control: the final objective is to design a pure force control of the system, in order to guarantee that each system element takes part in the thrust generation. This has to be done in embedding the previous curvature-based gait control as a model-based guidance function in order to drive the force control around the desired gait. Another advantage of this hypothetical solution is that the necessary measurement inputs will be restricted to current driving the DC motors of the system. This warrants further research on this subject.

6. Mission Control

Among the challenges that face the designers of underwater vehicle systems, the following is of major importance: design a computer-based mission control system that will, (Oliveira, 1998):

i. enable the operator to define a vehicle mission in a high level language, and translate it into a mission plan,
ii. provide adequate tools to convert a mission plan into a mission program that can be formally verified and executed in real-time,
iii. endow an operator with the capacity to follow the state of progress of the mission program as it is executed, and modify if required.

The first point concerns the aggregation of the different elementary actions the robot is able to perform, in higher level primitives that the mission designer is organizing in

function of the mission requirements. Moreover, vehicles have to be programmed and operated by end-users that are not necessarily familiarized with the most intricate details of underwater system technology. Generally, the framework adopted builds on the key concept of *Vehicle Primitive*, which is a parameterized specification of an elementary operation performed by the vehicle. Vehicle Primitives are obtained by coordinating the execution of a number of concurrent *System Tasks*, which are parameterized specifications of classes of algorithms or procedures that implement basic functionalities in an underwater robotic system. Vehicle Primitives are in turn logically and temporally chained for more abstract *Mission Procedures*, which are executed as determined by *Mission Programs*, in reaction to external events.
At a second level, Vehicle Primitive can be embodied in a Petri net structure, analysed in order to extract the system properties. The determinism of the Petri net structure can then be guaranteed, in order to meet the desired performance requirements. Another necessary stage is the development of special software environments that provide the necessary tools to go through all the stages of mission programming, followed by automatic generation of target code that runs on the vehicle computer network.
The third point is related to the on-line Man-Machine Interface (MMI) that manages the communication between the machine and the operator, and requires covering different aspect, according to the user objectives. The *system designer* has to access to low level information in order to test and validate the material and software architectures. The *control developer* has to integrate and tune its solutions, in terms of navigation, guidance, control, path planning…The *low level mission controller designer* is proposing to combine different system tasks in order to implement new vehicle primitives. The end-user has to program the mission in understandable terms according to its scientific speciality. And at last, the MMI has to include the on line system supervision module according to the permanent communication capabilities, that should allow for in-line mission replanning.

7. Software and Hardware Architectures

The previous solutions are reliable if the system is equipped with a software architecture that allows for deterministically running the previous algorithms onboard the vehicle. Moreover, notice that the acoustic devices the vehicle is carrying are potentially interfering. The management of the sensors' recruitment is a low level problem that has to be explicitly considered, in order to guarantee the reliability of the measurements. This problem belongs of the *software engineering* field, and follows three main approaches. *Deliberative* or *supervised architectures* are based on planning and allows for reasoning and making prediction. *Behavioural* or *reactive architectures* allows for the system to continuously reacting to the situation sensed by the perception system. Finally, hybrid architectures are complementing the advantages of the two previous ones, limiting their drawback. Comparative studies have been reported in the literature with (Ridao et al., 1999), (Valanavis et al., 1997), (Coste-maniere et al., 1995) and (Arkin, 1998). Moreover, the determinism requirement imposes to deploy the previous algorithms on a real-time operating system (Linux-RTAI, QNX, VxWorks, Windows-RTX, MicroC/OS-II…) guaranteeing the execution time of the processes. The latency of computing, or induced by the Local Area Network (LAN) communications, should be explicitly considered from the control aspect. Nevertheless, this highly complex problem is generally neglected in over-dimensioning the electronics and medium capacity.

From the hardware aspect, the objective is to design a reliable technological target onto which all the previous solutions are uploaded. The increase in hardware computing capabilities and the decrease in power consumption makes possible to use distributed computing architecture onboard underwater systems, where consumption, reliability and robustness are key-problems. A distributed system can be composed by many processes running on different computers, working together to meet the desired functional requirements of the mission control system. The distributed processes are coordinated using Inter-Processes Communication (IPC) and synchronization mechanism that include semaphores, Fifos, mailboxes, etc. The benefits of distributed processing are (Alves *et al.*, 1999):

i. increased performance by executing processes in parallel,
ii. increased availability, because a process is more likely to have a resource available if multiple copies are available,
iii. increased reliability since the system can be designed to be faul-tolerant and then automatically recover from failures,
iv. increased adaptability and modularity, since parts can be added or removed,
v. expensive resources can be share.

Asynchronous processes communicate with each other by exchanging messages. A common approach to distributed processing uses Local Area Network (LAN) to connect group of nodes together. Every node in the network can work alone as well as communicate with other nodes over the network to transfert data and/or synchronisation messages. Then, an application running on a local node can use resources of a remote node. Ideally, in distributed processing environments, the access to remote resources should be transparent. Different network topologies and communication strategies can be used to connect the different nodes of the architecture. For more information on this subject, please refer to (Alves *et al.*, 1999), (Halsall, 1996) and (Bennet, 1994), and for specific application on underwater systems, (Caccia *et al.*, 1995).

8. Conclusion

This paper surveyed the current state-of-the-art in the area of the underwater robotics, focusing on the Modelling, Navigation, Guidance and Control aspects. The problems of Mission Control and Software Architecture are key questions belonging to the Software Engineering domain and were briefly mentioned. Adding the Hardware Architecture question, these 7 points constitute the set of sub-problems, to be solved according to specific criteria and design methods, in order to realize a reliable system with guaranteed performances. The diversity of missions in which UUVs can be used, necessitates developing modular and reconfigurable vehicles, equipped on demand, and the capability to take place in a flotilla where the collaborative work brings new constraints.

Underwater robotics involves a complete set of theoretical problems, warranting long hours of exciting investigations. Moreover, the recent needs have pushed the development of new systems affording users advanced tools for ocean exploration and exploitation. The domain of underwater robotics is intended to grow rapidly, and the time where autonomous marine vehicles will freely roam the ocean is imminent.

As for any robotics application, one of the most important questions concerns the system reliability, in order to provide the necessary confidence before letting these vehicles go on populated routes. This problem impacts on the entire system, and we presented some solutions in order to guarantee the system performances.

Nevertheless, besides the robotics aspect, various problems have to be simultaneously considered, from network communication capabilities (between vehicles or infrastructure), via the energetic and sensing aspects, to the adaptation of the maritime legislation and public acceptation. These last two points may be the most difficult ones, but guess that the importance of the related issues will motivate the decision makers to provide rapid answers, and support emergent solutions.

9. References

Alves, J. ; Silvestre, C. & Pascoal, A. (1999). A distributed Architecture for Real Time Control. *Internal Report from the IST/ISR*, Lisbon, Portugal, January.

Arkin, R. (1998). *Behaviour-Based Robotics*. The MIT Press.

Aucher, M., (1981). *Dynamique des sous-marins*. Sciences et Techniques de l'Armement, 4° fascicule (in french), France.

Barraquand, J.; Langlois, B. & Latombe J. (1992). Numerical Potential Field Techniques for Robot Path Planning. *In the IEEE Transaction on System, Man and Cybernetics*, Volume 22, No 2, pp. 224-241, March.

Bennet, S. (1994). *Real-Time Computer Control, an Introduction*. Series in System and Control Engineering, Prentice Hall International, UK.

Blake, R. (2004). Review paper: fish functional design and swimming performance. *In the Journal of Fish Biology*, Blakwell publishing, Volume 65, Issue 5, pp 1193-1222, November.

Boyd, S.; El Ghaoui, L.; Feron, E. & Balakrishnan B. (1994). Linear Matrix Inequalities in Systems and Control Theory. *In SIAM Studies in Applied Mathematics*, Philadelphia.

Brian, D.; Andersen, O. & Moore, J. (1989). *Optimal Control: Linear Quadratic Methods*. Prentice Hall, London.

Brown, R. & Hwang P. (1992). *Introduction to Random Signals and Applied Kalman Filtering*. 2nd Ed., John Willey and Sons Inc.

Brown R. (1972). Integrated Navigation Systems and Kalman Filtering: a perspective. *In the journal of the Institute of Navigation*, Volume 19, No 4, pp. 355-362.

Caccia, N.; Virgili, P. and Veruggio, G. (1995). Architectures for AUVs: a Comparative study of Some Experiences. *In Proceedings of the AUV'95 International Symposium and Exhibition*. Washington D.C., USA, pp. 164-178.

Coste-Manière, E.; Wang H. and Peuch A. (1995). Control Architectures: What's going on? *In Proceedings of the US-Portugal Workshop on Undersea Robotics and Intelligent Control*, Lisbon, Portugal, Published by the University of S.W. Louisiana, USA, March, pp. 54-60.

Faltinsen, O. (1995). *Sea Loads on Ships and Ocean Structures*. Cambridge University Press.

Fan, Z.; Chen, J.; Zou, J. & Bullen, D. (2002). Design and fabrication of artificial lateral line flow sensors. *In the Journal of Micromechanics and Microengineering*, IOP Publishing, UK, Volume 12, pp. 655-661.

Fossen, T. (2002). *Marine Control Systems*. Marine Cybernetics Ed., Trondheim, Norway.

Fraisse P., Lapierre L., Dauchez P., Pierrot F., (2000) '*Position/Force Control of an Underwater Vehicle Equipped with a Robotic Manipulator*', SYROCO'00 Vienna, Austria, Sept.

Gillis, G. (1998). Environmental effects on undulatory locomotion in the america, eel Anguilla Rostrata: kinematics in water and on land. *In the Journal of Experimental Biology*, Edited by The Compnay of Biologist, UK, Volume 201, pp. 949-961.

Goldstein, R. (1976). *Fluid Mechanics Measurements*. Hemisphere Publishing Corporation, 1st Ed.

Gonzalez, L. (2004). *Design, Modelling and Control of an Autonomous Underwater Vehicle*. Bachelor of Engineering Honours Thesis, University of Western Australia, Wattke Grove, Australia.

Halsall, F. (1996) *Data Communications, Computer Networks and Systems*. 4th Edition, Addison-Wesley, Harlow, UK.

Hespanha, J.; Liberzon, D. & Morse, A. (1999). Logic based switching control of a non-holonomic system with parametric modelling uncertainties. *In the System and Control Letters, special issue on Hybrid Systems*, 38(3), 167-177.

Ijspeert, A. (1995). Locomotion Vertebrate. *In the Handbook of Brain and Neural Networks*, 2nd Edition, M. Arbib Ed., MIT Press, June.

Jouvencel, B.; Creuze, V. & Baccou, P. (2001). A new method for multiple AUV coordination: a reactive approach**.** *In the proceedings of the 8th IEEE International Conference on Emerging Technologies and Factory Automation*, Antibes-Juan les Pins, France.

Kaminer, I.; Kang W.; Yakimenko O. & Pascoal A. (2001). Application of Nonlinear Filtering to Navigation System Design Using Passive Sensors. *In IEEE Transaction on Aerospace and Electronic Systems*, Volume 37, No 1, October.

Khalil H.. (2002). *Nonlinear systems' third edition Prentice Hall*, New Jersey, USA.

Koditschek, D. (1987). Exact Robot Navigation by Means of Potential Functions: some Topological Considerations. *In the proceedings of the IEEE International Conference on Robotics and Automation*, Raleigh, North Carolina, USA.

Krstić, M.; Kanellakopoulos & Kokotovic, P. (1995). *Nonlinear and Adaptive Control Design*. John Willey & Sons, Inc., New York, USA.

Lapierre, L. (1999). *Etude et réalisation de la commande hybride position/force d'un robot équipé d'un bras manipulateur.* Ph. D. Thesis, Montpellier, France, November (In French).

Lapierre, L.; Fraisse, P. & M'Sirdi N. (1998). Hybrid Position/Force Control of a ROV with a Manipulator. *In the Proceedings of OCEAN'S 98* , Nice, France, September.

Lapierre, L. & Jouvencel, B. (2005). Path Following Control of an Eel-like Robot. *In the Proceedings of Oceans Europe 2005 Conference*, Brest, France, 20-23 June.

Lapierre[a], L.; Fraisse, P. & Dauchez, P. (2003). 'Position/Force Control of an underwater mobile manipulator. *In the Journal of Robotic System (JRS)*, Volume 20, Number 12, December, pp.707-722.

Lapierre[b], L. & Soetanto, D. (2006). Robust Nonlinear Path Following Control of an AUV. *Submitted to the IEEE Journal of the Oceanic Engineering Society*, January.

Lapierre[b], L.; Soetanto, D. & Pascoal, A. (2006). Non-Singular Path-Following Control of a Unicycle in the Presence of Parametric Modeling Uncertainties. *Accepted for publication in the Willey Journal on Robust and Nonlinear Control*, March.

Lapierre[c], L.; Creuze, V. & Jouvencel, B. (2006). Robust Diving Control of an AUV. *In Proceedings of the 7th IFAC MCMC'06 Conference*, Lisbon, Portugal, 20-22 September.

Louste, C. & Liegeois A. (1998). Robot Path Planning Using Models of Fluid Mechanics. *In Progress in Systems and Robot Analysis and Control Design*, Springer, EURISCON'9, ch. 41, pp. 515-524.

McIsaac, K. & Ostrowski, J. (2002). Experiments in closed loop control for an underwater eel-like robot. *In the proceedings of the IEEE International Conference on Robotics and Automation, ICRA'02*, Washington DC, USA, May, pp. 750-755.

Naeem, W.; Sutton, R. and Ahmad, M. (2003). LQG / LTR control of an autonomous underwater vehicle using hybrid guidance law. *In proceedings of the GCUV'03 Conference*, pp 35-40, April, Newport, UK

Naeem, W.; Sutton, R.; Ahmad, S. & Burns, R. (2003). A Review of Guidance Laws Applicable to Unmanned Underwater Vehicles. *In the Journal of Navigation*, 56(1), pp. 15-29.

Neal, M. (2006). A hardware proof of concept of a sailing robot for ocean observation. *Accepted for publication in the IEEE Journal of Oceanic Engineering*. URL: http://hdl.handle.net/2160/24

Nettleton, E.; Durrant-Whyte H.; Gibbens P. & Goktogan A. (2000). Multiple platform localisation and building. *In Proceedings of Sensor Fusion and Decentralised Control in Robotics Systems III*, Vol. 4196, pages 337-347, November.

Newmann, J. (1977). *Marine Hydrodynamics.* Cambridge, MIT Press, 1st ed.

Nieto, J.; Guivant, J. & Nebot, E. (2003). Real-time Data Association for FastSLAM. *In the proceedings of the IEEE International Conference on Robotics and Automation*, Taipei, Taiwan, September 14-19.

Latombe, J. (1991). *Robot Motion Planning*. Kluwer Academic Pub.

Oliveira, P.; Pascoal, A.; Silva V. & Silvestre C. (1998). Mission Control of the Marius AUV: System Design, Implementation, and sea Trials. *In the International Journal of Systems Science, Vol. 29, No. 10*, pages 1065-1080.

Oliveira, P. (2002). *Periodic and Non-linear Estimators with Applications to the Navigation of Ocean Vehicles*. Ph. D. Thesis, Lisbon, Portugal, June.

Parodi, O.; Lapierre, L. & Jouvencel, B. (2006). Optimised Gait for Anguiliform Locomotion. *In Proceedings of the OCEANS'06 Conference*, Singapore, 16-19 May, 2006.

Pascoal, A.; Kaminer, I. & Oliveira, P. (2000). Navigation System Design Using Time-Varying Complementary Filters. *In the IEEE Transaction on Aerospace and Electronic Systems*, Volume 36, No 4, October.

Pere, R.; Battle, P.; Amat, J. & Roberts, J. (1999). Recent Trends in Control Architectures for Autonomous Underwater Vehicles. *International Journal of System Sciences*, Volume 30, No 9, pp. 1033-1056

Perrier, M. (2005). The visual servoing system "CYCLOPE" Designed for Dynamic Stabilisation of AUV and ROV. *In the Proceedings of the OCEANS Europe 2005 Conference*, Brest, France, June.

Prado, M. (2004). *Modelização e Controlo de um Veículo Oceanográphico Autónomo.* Master Science Thesis, Lisbon, Portugal, June (in Portuguese).

Rolfes, S. & Rendas, M. (2001). Statistical Habitat Maps For Robot Localisation in unstructured environments. *In the Proceedings of the IEEE / MTS OCEANS'01 Conference*, Honolulu, Hawaii, U.S.A, 5 – 8 November 2001

Saintval, W. (2002). Optimizing Robotic Aquatic Locomotion. *In the Proceedings of the 34th Annual Meeting of the Florida Section of the Mathematical Association of America*, D. Kerr and B. Rush Editors, Florida, USA, April.

Samson, C. & Ait-Abderrahim, K. (1991). Mobile Robot Control Part 1 : Feedback Control of a Nonholonomic Robot. *Technical report N° 1281*, INRIA, Sophia-Antipolis, France, June.

Sagatun, S.; Fossen, T. & Lindegaard, K. (2001). Inertance Control of Underwater Installation. *In Proceedings of the 5th IFAC Conference on Control Application in Marine Systems (CAMS'01)*, Glasgow, U.K..

Sfakiotakis, M. & Tsakiris, D. (2004). A simulation Environment for Undulatory Locomotion. *In the proceedings of the Applied Simulation and Modelling Conference (ASM'04)*, Rhodes, Greece, June 28-30.

Silvestre, C. (2002). *Multi objective optimization theory with applications to integrated design of controllers / plants for autonomous vehicle.*, Ph. D. thesis, June, Lisbon, Portugal.

Silvestre, C.; Pascoal, A. and Kaminer, I. (2002). On the design of Gain-Scheduled trajectory tracking controllers. *In the International Journal of Robust and Nonlinear Control*, 12:797-839.

Slotine J. (1991). *Applied Nonlinear Control*, Prentice Hall, London, UK.

Soetanto, D.; Lapierre, L. & Pascoal, A. (2003). Adaptive Non-singular path-following control of dynalic wheeled robot. *In the Proceedings of the ICAR Conference*, Coimbra, Portugal, June.

Tytell, E. (2003). The Hydrodynamics of eel swimming II. Effect of swimming speed. *In the journal of Experimental Biology*, Volume 207, Published by the Company of Biolologists, August, pp. 3265-3279.

Vaganay, J.; Jouvencel, B.; Lepinay, P. & Zapata, R. (1988). Taipan an AUV for very shallow water applications. *In the Proceedings of World Automation Congress (WAC'98)*, San Diego, USA.

Valanavis, P.; Gracanin, D.; Matijasevic, M. ; Kolluru, R. & Demetriou, G. (1997). Control Architecures for Autonomous Underwater Vehicles. *In IEEE Control Systems Magazine*, pp. 48-64

Whitcomb, L. & Yoerger D. (1995). Comparative Experiments in the Dynamics and Model-Based Control of Marine Thrusters. *In Proceedings of the IEEE Oceans'95 Conference*, San Diego, USA.

Webber, D.; Boutilier, R.; Kerr, S. & Smale, M. (2001). Caudal differential pressure as a predictor of swimming speed of cod (*Gadus Morhua*). *In the Journal of Experimental Biology*, Edited by the Compnay of Biologists, Volume 204, pp 3561 – 3570.

Zapata, R.; Cacitti, A. & Lépinay, P. (2004). DVZ-Based Collision Avoidance Control of Nonholonomic Mobile Manipulator. *JESA, European Journal of Automated Systems*, Volume 38, No 5, pp. 559-588.

Mobile Robots: towards New Applications

Edited by Aleksandar Lazinica

ISBN 978-3-86611-314-5
Hard cover, 600 pages
Publisher I-Tech Education and Publishing
Published online 01, December, 2006
Published in print edition December, 2006

The range of potential applications for mobile robots is enormous. It includes agricultural robotics applications, routine material transport in factories, warehouses, office buildings and hospitals, indoor and outdoor security patrols, inventory verification, hazardous material handling, hazardous site cleanup, underwater applications, and numerous military applications. This book is the result of inspirations and contributions from many researchers worldwide. It presents a collection of wide range research results of robotics scientific community. Various aspects of current research in new robotics research areas and disciplines are explored and discussed. It is divided in three main parts covering different research areas: Humanoid Robots, Human-Robot Interaction, and Special Applications. We hope that you will find a lot of useful information in this book, which will help you in performing your research or fire your interests to start performing research in some of the cutting edge research fields mentioned in the book.

How to reference

In order to correctly reference this scholarly work, feel free to copy and paste the following:

Lapierre Lionel (2006). Underwater Robots Part II: Existing Solutions and Open Issues, Mobile Robots: towards New Applications, Aleksandar Lazinica (Ed.), ISBN: 978-3-86611-314-5, InTech, Available from: http://www.intechopen.com/books/mobile_robots_towards_new_applications/underwater_robots_part_ii__existing_solutions_and_open_issues

INTECH
open science | open minds

InTech Europe
University Campus STeP Ri
Slavka Krautzeka 83/A
51000 Rijeka, Croatia
Phone: +385 (51) 770 447
Fax: +385 (51) 686 166
www.intechopen.com

InTech China
Unit 405, Office Block, Hotel Equatorial Shanghai
No.65, Yan An Road (West), Shanghai, 200040, China
中国上海市延安西路65号上海国际贵都大饭店办公楼405单元
Phone: +86-21-62489820
Fax: +86-21-62489821